Marine Geology xxx (2009) xxx–xxx

Contents lists available at ScienceDirect

Marine Geology

journal homepage: www.elsevier.com/locate/margeo

The influence of sea level and tectonics on Late Pleistocene through Holocene sediment storage along the high-sediment supply Waipaoa continental shelf

Thomas P. Gerber [a,*], Lincoln F. Pratson [a], Steve Kuehl [b], J.P. Walsh [c], Clark Alexander [d], Alan Palmer [e]

[a] Nicholas School of the Environment and Earth Sciences, Old Chemistry Box 90227, Duke University, Durham, NC 27708, USA
[b] Virginia Institute of Marine Sciences, Rt.1208, Greate Road, P.O. Box 1346, Gloucester Point, VA 23062, USA
[c] Department of Geological Sciences, East Carolina University, Room 101 Graham Building, Greenville, NC 27858, USA
[d] Skidaway Institute of Oceanography, 10 Ocean Science Circle, Savannah, GA 31411, USA
[e] Soil and Earth Sciences, Institute of Natural Resources, Private Bag 11 222, Palmerston North, New Zealand

ARTICLE INFO

Available online xxxx

Keywords:
Waipaoa shelf
stratigraphy
transgression
highstand
accumulation rates

ABSTRACT

We present geophysical and core evidence showing how subsidence caused by forearc shortening has accommodated Late Pleistocene and Holocene sediments supplied to the tectonically active Waipaoa shelf (NZ), limiting off-shelf export during the early sea level highstand. The last glacioeustatic fall and subsequent rise exposed and then flooded a shelf segmented into subbasins separated by zones of uplift, leaving key stratigraphic markers of shoreline regression and transgression that vary strongly in character across the shelf. Highstand sediment isopachs tied to piston cores dated using tephra correlation and a radiocarbon age model provide a sediment budget at ~2000 yr intervals from the mid-Holocene (~5500 cal. yr BP) to present. Sediment load estimates from our shelf budget are in agreement with published model estimates for suspended sediment discharge from the Waipaoa River for the past 3000 yr but, importantly, do not show the 6-fold increase in the Waipaoa's sediment output that began with human settlement 700 yr ago and accelerated with deforestation over the last century. Bypassing of Waipaoa sediment to the slope may therefore be a recent phenomenon caused by unnaturally high sediment loads, a conclusion supported by data reported elsewhere in this volume. Our study also reveals evidence for (1) a relatively thick mid-shelf transgressive section deposited during the last eustatic rise that may correlate to estuarine sequences reported from numerous sites on the modern coastline of the North Island, (2) a slight decrease in total basin filling rates during the highstand, and (3) variability in the partitioning of highstand sediments between individual subbasins that may reflect differing degrees of tectonic accommodation.

1. Introduction

Continental shelves are broadly defined by the landward and seaward extent of shoreline movement during relative sea level change. So strata formation and preservation on shelves is complicated by the fact that their surfaces are subject to subaerial, coastal, and marine sediment transport. In the source-to-sink perspective advocated in this issue, shelves are part of a marine sediment pathway extending from the shoreline to abyssal depths, and modulate when, how, and in what amount sediment delivered to the shoreline ultimately moves beyond the shelf break. Quantifying sediment delivery to, storage in, and export from continental shelves is therefore a key component of a more complete source-to-sink picture of margin sedimentation.

The primary controls on shelf sedimentation are expressed in sequence stratigraphy, which relates the balance of relative sea level (eustasy plus sea floor movement) and sediment supply to the formation of continental margin strata (Mitchum et al., 1977; Vail et al., 1977; Wilgus et al., 1988, and references therein). Relative sea level determines the rate at which accommodation space is created or destroyed in a basin, while sediment supply determines the rate at which it can fill. Eustasy superimposed upon a margin-wide pattern of basement subsidence determines accommodation on most passive margins, but on active margins both localized uplift and subsidence associated with convergent deformation can modulate the eustatic control on accommodation.

In essence, sequence-stratigraphic analyses seek to subdivide margin strata into sequences by identifying distinct bounding surfaces that bear the signature of shoreline movement (Posamentier and Allen, 1999). Of particular interest are strata formed under known eustatic (global) variation, because the signature of local factors (principally sediment supply and tectonics) on sequences and bounding surfaces can be recognized and used to guide interpretations of seismic, core, or outcrop data from similar settings where none of the controlling factors is known (Naish and Kamp, 1997). In this regard, strata along convergent margins are particularly useful.

* Corresponding author. Present address: Chevron Energy Technology Company, 1500 Louisiana St., Houston, TX 77002, USA.
E-mail address: thomas.gerber@chevron.com (T.P. Gerber).

0025-3227/$ – see front matter © 2009 Elsevier B.V. All rights reserved.
doi:10.1016/j.margeo.2009.10.002

Plio-Pleistocene sedimentation on continental margins has occurred during a period of Earth history in which glacioeustatic fluctuations are well-constrained (Pillans et al., 1998). On several convergent-margin coastlines, deformation across forearc basins has subaerially exposed thick shallow marine and paralic late Pliocene and early Pleistocene strata (Clifton et al., 1988; Haywick et al., 1992; Naish and Kamp, 1995). In the tectonically active forearc of the Hikurangi subduction margin along North Island, New Zealand, wide outcrop exposure of such sediments reveals eustatically-driven (10^5–10^4 yr) depositional sequences and bounding surfaces whose expression is characterized in terms of fine-scale (10^0–10^1 m) facies architecture (Fig. 1). Beneath adjacent modern shelves along the North Island East Coast are similar sequences driven by Late Pleistocene glacioeustasy (Lewis, 1973; Barnes et al., 2002), but their signature in seismic and core data of comparably high resolution is largely unexplored.

Shelves on convergent margins commonly collect sediments from steep, rapidly uplifting terrestrial catchments drained by rivers with high sediment loads. In the modern eustatic highstand, most are characterized by appreciable shelf sedimentation and thus fall into the "supply-dominated" regime of Swift and Thorne (1991). Whether early highstand, supply-dominated shelves trap most sediments supplied to them or bypass a significant fraction to continental slopes is an important question in deepwater sedimentation (Walsh and Nittrouer, 2003; Nittrouer, 1999), and ultimately depends on the magnitude of sediment supply relative to shelf accommodation (i.e., shelf width and subsidence). Determining this balance from the stratigraphic record is difficult because it requires sediment supplied to and stored on shelves to be independently quantified. Only where shelf accumulation has been significant and mappable during the late Holocene – an early highstand period when sediment supply can also be reasonably estimated from studying modern rivers – can the balance be quantified. Shelves draining the high-yielding catchments on the eastern North Island provide this opportunity.

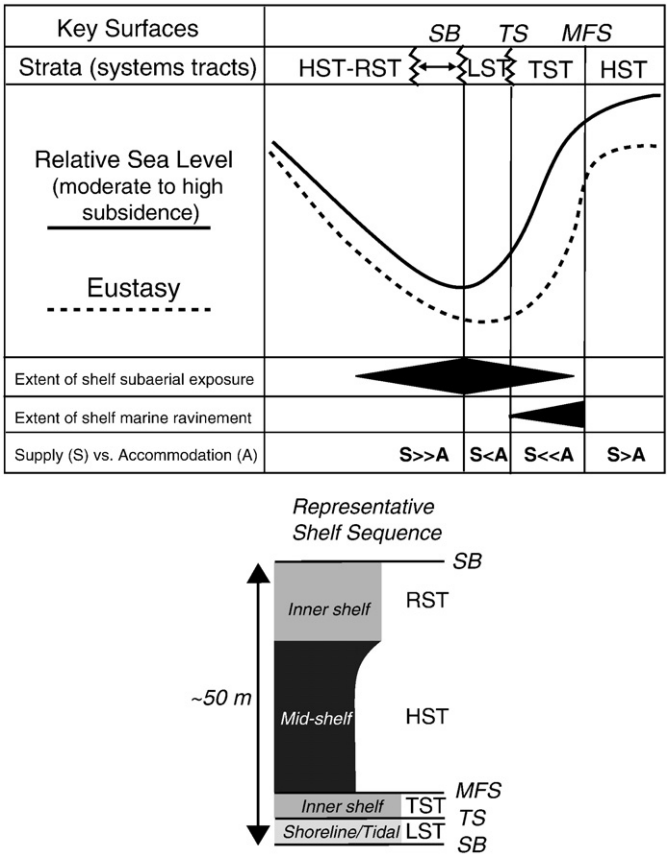

Fig. 1. Chart illustrating the timing of stratal-surface generation relative to sea level on the shelf (top) and a representative vertical log sequence (bottom), both based on the work of Haywick et al. (1992) on Plio-Pleistocene shallow marine strata exposed onshore from Hawke's Bay (NZ). Figure is adapted from Naish and Kamp (1997), with schematic sea level curves following the framework of Allen and Allen (2005). Sequence-stratigraphic terminology used here and elsewhere is defined as follows: HST — highstand strata, RST — regressive strata, LST — lowstand strata, TST — transgressive strata, SB — sequence boundary, TS — transgressive surface, MFS — maximum flooding surface.

The modern Waipaoa continental shelf lies in the Hikurangi forearc between Hawke's Bay and East Cape and accumulates sediments washed from a rapidly eroding terrestrial catchment (Fig. 2) (Foster and Carter, 1997; Orpin et al., 2006; Kuehl et al., 2006). In this paper, we combine high-resolution geophysical and core data from the Waipaoa shelf in pursuit of two primary results: (1) a subdivision of the most recent sedimentary sequence associated with the last glacioeustatic lowstand, rise, and modern highstand based on key stratigraphic surfaces and stratal patterns, and (2) a quantification of early highstand sediment storage that can be compared to long-term and short-term fluvial supply estimates to determine whether the Waipaoa shelf is an efficient trap for terrestrial sediment. In addressing these objectives, we refine existing interpretations for eustatic lowstand-to-highstand sedimentation on the Waipaoa shelf and highlight the importance of spatial variability in tectonic accommodation. Our millennial-scale highstand sediment budget is an important component of the larger source-to-sink budget for the Waipaoa margin, and provides a bridge between studies of short-term (last ~100–200 yr) shelf accumulation and long-term (last ~3000 yr) terrestrial sediment yields reported elsewhere. By establishing a baseline trapping efficiency for the entire shelf, we assess how a recent but sizable anthropogenic influence on land is affecting the storage of sediment offshore.

2. The Waipaoa sedimentary system (WSS)

2.1. The source

Sediment delivered to the Waipaoa continental shelf is sourced primarily from the 2200 km^2 Waipaoa River Basin (Fig. 2). The catchment lies along the flanks of New Zealand's Raukumara Range, which is part of the volcanic arc associated with subduction of the Pacific Plate beneath the North Island. High (~1–2 mm yr^{-1}) rates of subduction-driven uplift in the headwaters (Berryman et al., 2000; Litchfield and Berryman, 2007), highly erodible Cretaceous-to-Pliocene aged sedimentary rocks underlying the catchment (Mazengrab and Speden, 2000), moderate but episodically intense rainfall (Foster and Carter, 1997), periodically large subduction-zone earthquakes (Lewis, 1980), and tephra-producing volcanic eruptions (Wilmshurst and McGlone, 1996; Kettner et al., 2007) all favor high natural sediment yields from the basin. Hillslope gullying and, when rainfall intensity is high, shallow landsliding dominate catchment erosion (Page et al., 1999; Hicks et al., 2000; Reid and Page, 2003; Hicks et al., 2004).

Sediment production and delivery to catchment channels was higher during the last glacial maximum (Berryman et al., 2000), and storm-induced landsliding may have become more frequent with the onset of an ENSO-dominated climate during the mid-Holocene (Gomez et al., 2004). Erosion today is amplified by the almost complete removal of indigenous forest cover that began with human settlement 700 cal. yr BP and accelerated during the 19th and 20th centuries (Gage and Black, 1979; Foster and Carter, 1997).

The Waipaoa River is predominantly gravel-bedded, with bedrock tributaries in the headwaters and a gravel–sand transition that today lies only 8 km from the coast (Rosser, 1997). The anthropogenic influence on modern sediment production is manifest in aggradation of channel beds through much of the catchment and an extraordinarily high suspended sediment output to the coast, which at

Please cite this article as: Gerber, T.P., et al., The influence of sea level and tectonics on Late Pleistocene through Holocene sediment storage along the high-sediment supply Waip..., Mar. Geol. (2009), doi:10.1016/j.margeo.2009.10.002

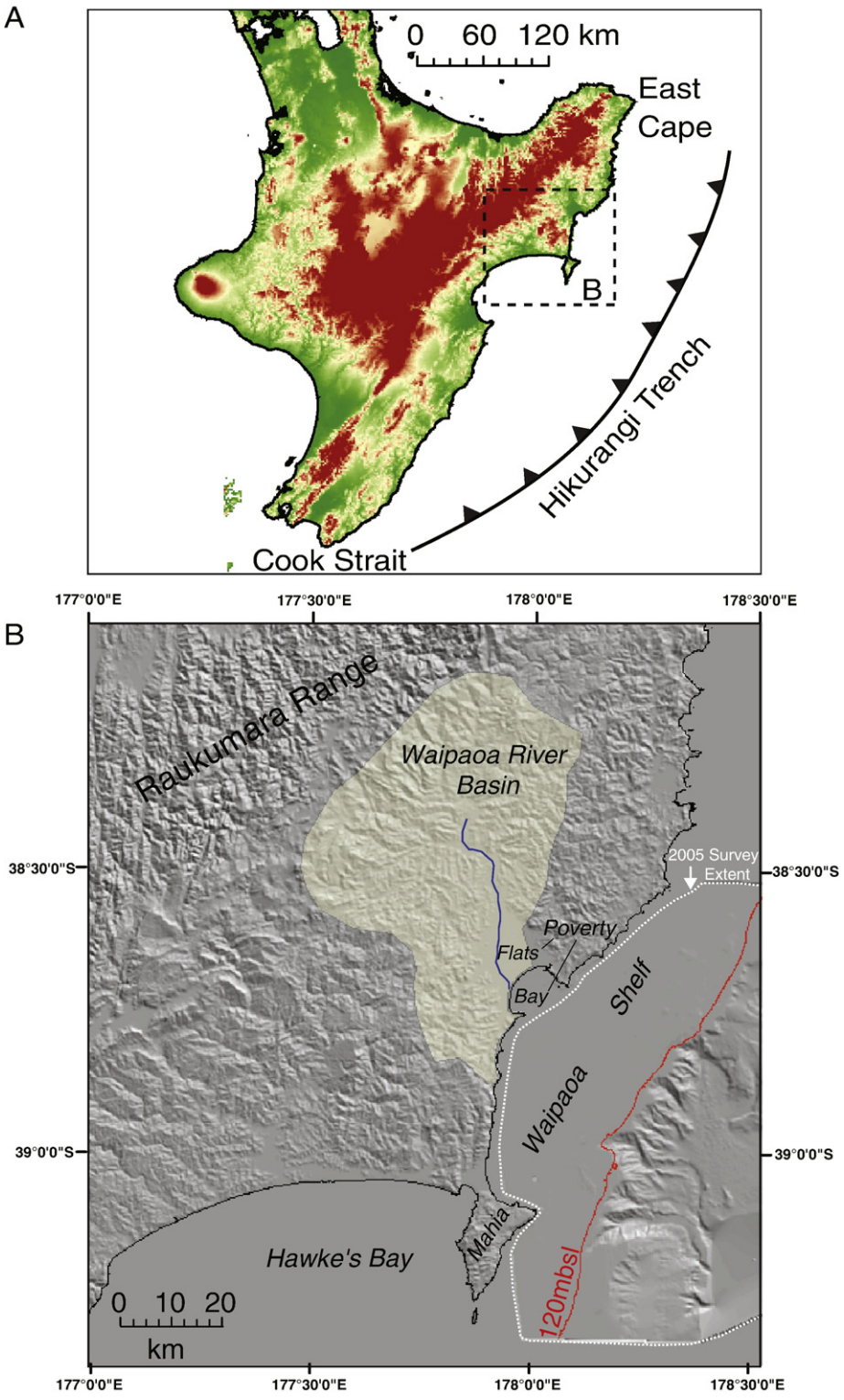

Fig. 2. A) Elevation map of North Island, New Zealand. B) Shaded relief map of Waipaoa catchment and continental margin. Key features outlined are: Waipaoa drainage basin (2200 km^2), Waipaoa lower coastal plain (Poverty Plats), Poverty Bay, Waipaoa continental shelf, Mahia Peninsula, and the 120 mbsl isobath near shelf edge. Projection in this and all subsequent maps is based on the UTM coordinate system (Zone 60S, WGS 84).

15 Mt yr^{-1} translates to one of the highest specific sediment yields in the world (6750 t km^{-2} yr; Hicks et al., 2000; Orpin et al., 2006). Prehistoric river sediment loads are not well understood, particularly during the immediate post-glacial and early Holocene period when climate and sea level rise triggered rapid long-profile adjustment of the Waipaoa mainstem and its tributaries, evidenced today by the presence of knickpoints and both cut and fill terraces (Berryman et al., 2000; Crosby and Whipple, 2006). A record of post-glacial sediment storage beneath the alluvial plain of Poverty Flats (Fig. 2) and a series of beach ridges inland from the modern coast provide a history of shoreline movement during the Holocene transgression and subsequent highstand (Brown, 1995).

Since eustatic sea level stabilized at ~7000 cal. yr BP (Gibb, 1986), coastal accretion of sand delivered in the Waipaoa's bedload has

Please cite this article as: Gerber, T.P., et al., The influence of sea level and tectonics on Late Pleistocene through Holocene sediment storage along the high-sediment supply Waip..., Mar. Geol. (2009), doi:10.1016/j.margeo.2009.10.002

sustained shoreline progradation into Poverty Bay while large volumes of mud have been exported to the Waipaoa shelf (Foster and Carter, 1997). Recently, Kettner et al. (2007) used a semi-empirical quantitative model to estimate suspended sediment output from the Waipaoa's catchment for the last 3000 yr. Their results put the modern Waipaoa load in perspective, showing a ~6-fold increase in suspended sediment discharge with settlement and forest clearing in the catchment headwaters. Modern suspended sediment dispersal through and beyond Poverty Bay is a subject of active research (see Wood and Carter, Carter and Gomez, this issue) but is not dealt with here.

2.2. The sink

The Waipaoa continental shelf and slope lie immediately inboard of the Hikurangi subduction zone (Fig. 2). Landward of the trench, active deformation has produced an imbricated accretionary prism beneath the modern continental slope. The slope is segmented by thrust faulting into ridges and mini-basins, and large-scale mass failures are documented (Orpin, 2004; Orpin et al., 2006). Readers are referred to studies by Bodger et al., Walsh et al., and Alexander et al. appearing elsewhere in this issue for more detailed studies of deformation and sedimentation on the Waipaoa slope.

The most landward emergent thrust in the deformation front marks the edge of the continental shelf and the forearc basin beneath (Lewis, 1980; Lewis and Pettinga, 1993). Sustained forearc subsidence from rotation of emergent outer shelf structures accommodates Quaternary syntectonic growth strata, similar to that documented to the south of the Waipaoa margin in Hawke's Bay (Lewis, 1973; Barnes et al., 2002). Subsidence gives way to uplift along much of the Waipaoa coastline, where Quaternary shorelines are mapped well-above modern sea level (Ota et al., 1988; Berryman, 1993a,b). Pioneering work by Foster and Carter (1997) documented a continuous sequence of latest Pleistocene and Holocene growth strata on the Waipaoa shelf, demonstrating active syntectonic accumulation there. In the analysis that follows, we use newly acquired high-resolution seismic and core data to present a more detailed stratigraphy of this sequence.

3. Data and methods

Seismic and bathymetric data reported below were obtained during two consecutive cruises aboard the R/V *Kilo Moana* to map the Waipaoa shelf and slope as part of the NSF MARGINS Source-to-Sink program. Bathymetric data from the shelf and slope were collected with shallow and deepwater multibeam echosounders (EM1002 and EM300, respectively). Full swath coverage was only achieved over the Waipaoa outer shelf, with a maximum grid resolution of 5 m (see Walsh et al., 2007). Due to more sparse coverage over the inner and middle shelf, bathymetric grids shown here were regrid via interpolation to 200 m pixel resolution (Fig. 3).

We collected over 1800 km of high-resolution chirp seismic data from the shelf with an EdgeTech 512c subbottom profiler (Fig. 3). We used an FM pulse swept over 30 ms from .5 to 7.2 kHz, and sampled returns at 64 μs intervals. Once digitized, the data were match filtered for pulse compression and stored in analytic form. The combination of high bandwidth, long pulse duration, and the hydrophone directionality in the chirp system ensure high resolution, high signal-to-noise ratio, and diminished sidelobes from dipping reflectors off the sonar's vertical axis (Schock et al., 1994). As a result, no post-processing is required to obtain interpretable seismic sections. Maximum penetration is

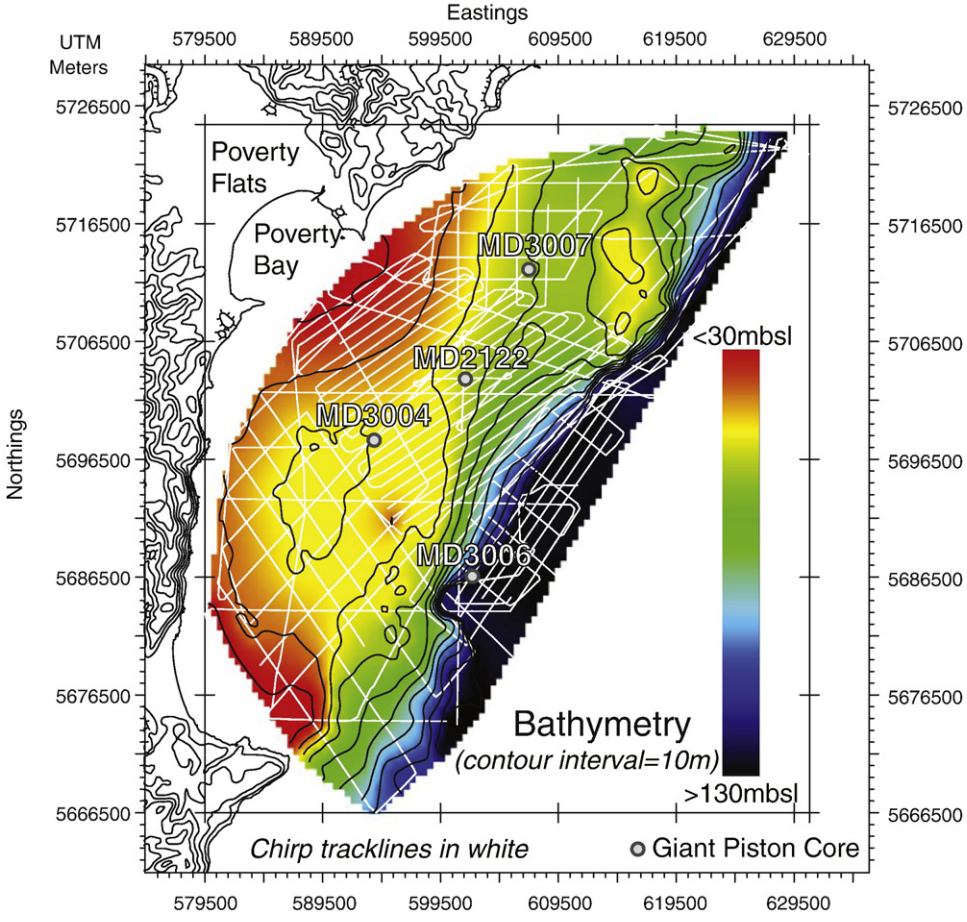

Fig. 3. Bathymetric map of Waipaoa continental shelf and upper most slope. Geophysical tracklines (chirp, multibeam) are shown in white along with piston core sites.

Please cite this article as: Gerber, T.P., et al., The influence of sea level and tectonics on Late Pleistocene through Holocene sediment storage along the high-sediment supply Waip..., Mar. Geol. (2009), doi:10.1016/j.margeo.2009.10.002

attenuation dependent and thus varies by substrate, but can exceed 100 m in gas-free fine muds. Unless noted otherwise, all chirp profiles shown here are presented as the signal envelope, or instantaneous amplitude.

A second MARGINS-supported effort was undertaken during the 2006 MATACORE cruise aboard the R/V *Marion Dufresne* to recover 5 giant piston cores from the Waipaoa middle and outer shelf. Data from three long cores, each targeting one of three distinct depocenters identified in the chirp data, are reported here: MD3004, MD3006, and MD3007, collectively referred to as the 'MD06' cores (locations in Fig. 3). Before the cores were split, onboard measurements of gamma bulk density, p-wave velocity, and magnetic susceptibility were recorded at 2 cm intervals using a GEOTEK Multi Sensor Core Logger (MST). Effective porosities were calculated from the wet bulk densities assuming normal seawater salinity (1030 $kg\,m^{-3}$) and solid grain density of 2650 $kg\,m^{-3}$. Subsequently, cores MD3004 and MD3007 were split, described, photographed, selectively subsampled, and archived for ongoing analyses. The first coring attempt adjacent to the MD3007 site recovered core MD3001. This core was disturbed upon recovery, particularly in its middle and lower sections, which prevented complete MST logging. Still, tephras collected in the upper segment of the core corroborate the chronology for MD3007. MD3006 was split but not described or photographed on board due to time constraints. However, photographs and descriptions from a shorter test core (MD3005) adjacent to it were obtained and show two prominent tephra beds that we assume also appear in MD3006. Published data from an existing long piston core (MD2122) was also used for correlation (Gomez et al., 2004). Further details on the coring campaign are summarized by Proust et al. (2006).

Mappable reflectors in the chirp records were digitized manually as horizons and then gridded with a nearest neighbor algorithm to produce surfaces for isopaching and/or structure mapping. Interpolation was required on older horizons that descended below areas in the deepest zones of the basin acoustically obscured by gas. Time-depth relationships for core sites MD3004, MD3006, and MD3007 were estimated using synthetic seismic traces to correlate prominent reflection events with high impedance (i.e., bulk density*p-wave velocity) contrasts observed in the core MST records. The adjusted time-depth relationships facilitate correlation of time-marker horizons between cores on the seismic profiles.

The shelf-wide sediment budget for cored intervals bounded by time-marker horizons was established using isopachs grids and the core porosity curves for MD3004, MD3006, and MD3007. The porosity-depth curves were fit to an Athy-type consolidation model, $\varphi(z) = \varphi_0 * \exp[-c*z]$, so that a unique coefficient c could be estimated for each core and extrapolated to the larger depocenter within which each was located. For each isopach grid, pore volumes per unit area were computed by integrating the consolidation curve over the corresponding depth interval at each grid cell (200×200 m). Total solids for each isopach were then computed from the summed pore volume, summed total volume, and an assumed grain density of 2650 $kg\,m^{-3}$. For depth isopachs and structure maps extending below the cored interval, a nominal sound speed of 1500 $m\,s^{-1}$ was assumed. Average accumulation rates in the sediment budget are all

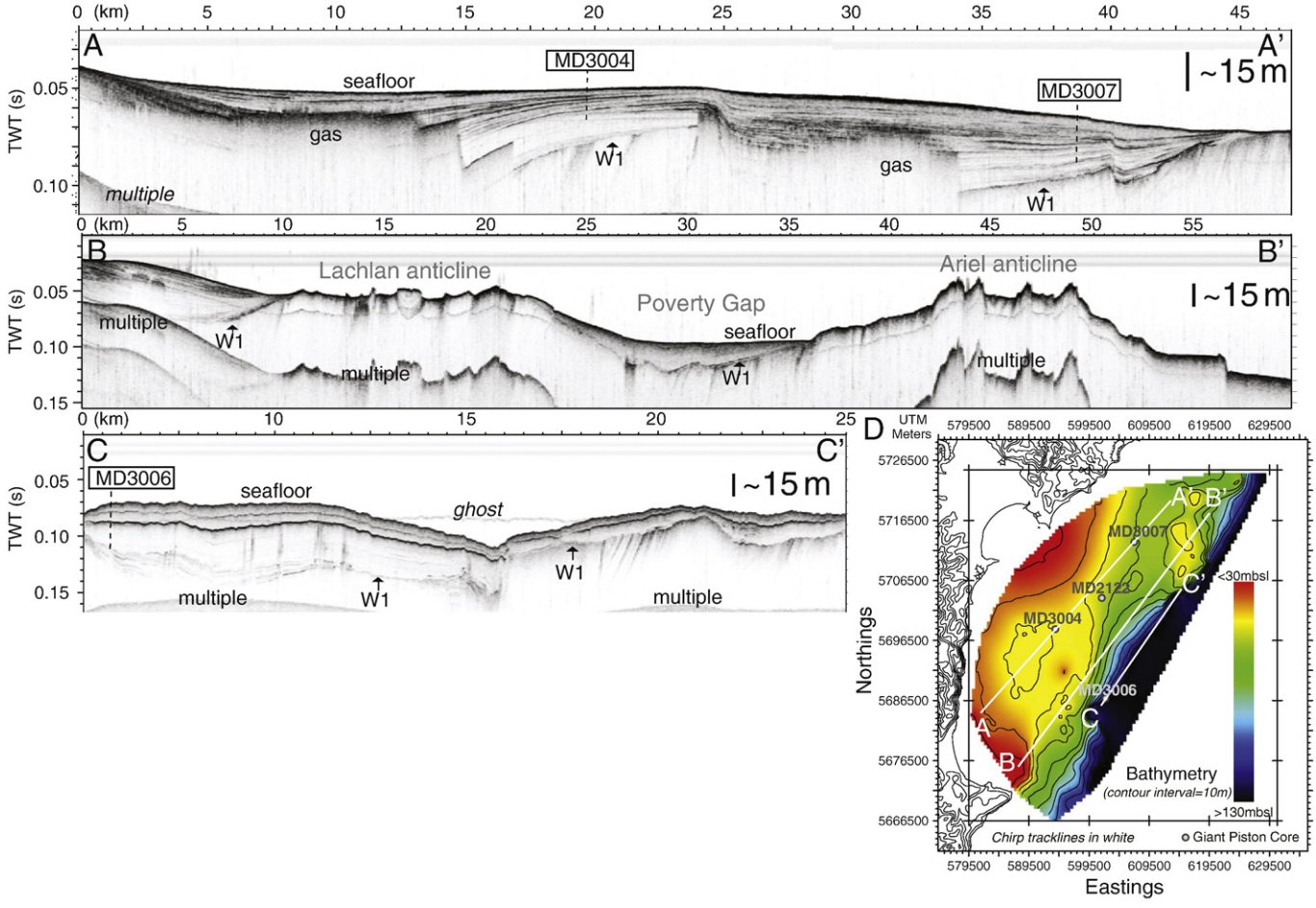

Fig. 4. Three seismic strike lines (A–C) crossing the Waipaoa middle and outer shelf at the locations shown on the inset bathymetric map (D). The seismic trace envelopes are plotted (instantaneous amplitude) in two-way travel time (TWT); an approximate depth scale in meters is shown assuming a sound velocity of 1500 $m\,s^{-1}$. Note the horizontal scale is in kilometers. Piston core locations are also shown on the profiles. Lachlan and Ariel anticlines, along with Poverty Gap, are labeled in gray in (B).

Please cite this article as: Gerber, T.P., et al., The influence of sea level and tectonics on Late Pleistocene through Holocene sediment storage along the high-sediment supply Waip..., Mar. Geol. (2009), doi:10.1016/j.margeo.2009.10.002

reported with a fixed, 10% uncertainty to account for several potential sources of error that are not quantifiable.

4. Waipaoa shelf stratigraphy

4.1. Overview of Late Pleistocene and Holocene seismic architecture

Interpreting a limited set of 3.5 kHz profiles crossing the Waipaoa margin, Foster and Carter (1997) identified distinct middle and outer shelf modern depocenters above the first prominent unconformity in the subsurface, which they interpreted as an erosion surface associated with the last sea level lowstand. Following Lewis (1973), who made the same interpretation of shelf strata south of Hawke's Bay (NZ), they labeled this horizon "W1", a convention we adopt here. In this section we describe the structure of W1 and the overlying sedimentary architecture using our newly acquired chirp records, before proceeding in Section 5 to develop a sequence-stratigraphic interpretation for the shelf strata.

The character of W1 and the strata above it are seen in three chirp lines that parallel the coast (Fig. 4A–C). In each, the W1 unconformity is defined by the loss of acoustic penetration into lower strata and is angular in sections where tilted bedding planes are observed beneath it. The two mid-shelf depocenters above W1 are separated by an emergent structure draped with thin syntectonic strata. Apparent uplift along this structure and the Mahia coast south of Poverty Bay define the syncline that contains a southern depocenter (Fig. 4A). Numerous reflectors there dip into a basin deep where gas obscures the W1 surface. Gas is also present at depth in a northern depocenter, but reflectors there are more parallel and converge northward onto a second emergent structure that exposes W1 at the seafloor.

Lewis and Pettinga (1993) and Foster and Carter (1997) identified these structures, Ariel (north) and Lachlan (south), as emergent anticlinal folds with cores of Miocene slope mudstone that mark the front of accretionary slope deformation. A chirp line parallel to but seaward of Fig. 4A crosses the crests of the two anticlines and terminates to the southwest on the uplifted Mahia coast (Fig. 4B). The anticlines are separated by a ~10 km offset known as Poverty Gap (Foster and Carter, 1997), where a thin, acoustically transparent unit drapes W1. A third line seaward of the anticline crests shows that the structural offset between them is partially accommodated along a fault visible seaward of the Lachlan structure. Strata in a third subbasin, described on 3.5 kHz profiles by Orpin et al. (2006), thicken across the hanging wall of this fault and extend to the northern rim of Lachlan canyon. The depocenter above W1 is relatively thick there, and is acoustically transparent except for two prominent, draping reflectors.

The structural configuration of the shelf is shown in Fig. 5 with a map of the W1 surface and in Fig. 6 with an isopach of the strata above it. Across the shelf, the thickness of overlying basin fill mirrors the deformation of W1, which shows greater negative relief in the

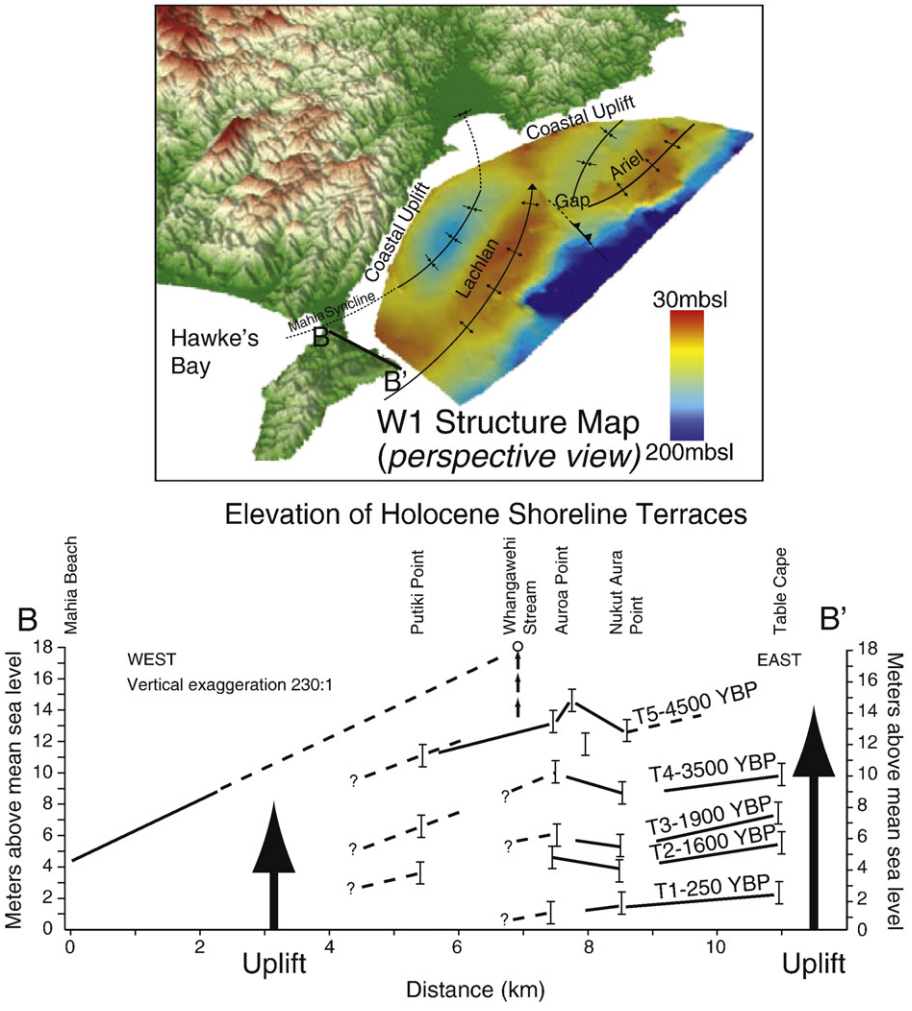

Fig. 5. (Top) Structure map of the W1 surface in perspective view, with the onshore digital elevation model (DEM) included. Major structural features discussed in text are labeled, along with the transect shown in bottom panel. (Bottom) Figure redrawn from Berryman (1993a,b) showing westward tilt of uplifted Holocene marine terraces on the northern coast of Mahia Peninsula. Note maximum uplift of ~4500 yr terrace is ~15 m.

Please cite this article as: Gerber, T.P., et al., The influence of sea level and tectonics on Late Pleistocene through Holocene sediment storage along the high-sediment supply Waip..., Mar. Geol. (2009), doi:10.1016/j.margeo.2009.10.002

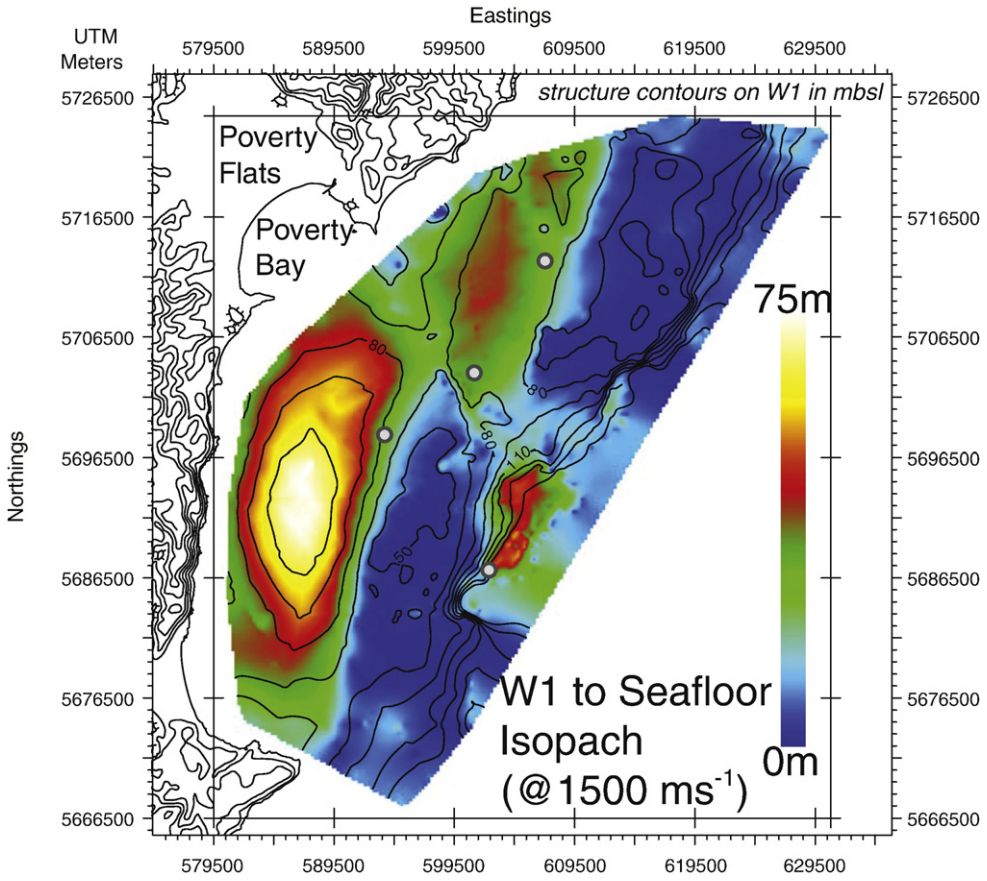

Fig. 6. Isopach map showing sediment thickness between W1 and the seafloor across the Waipaoa shelf assuming a velocity of 1500 m s^{-1}. Structure contours on the W1 surface (mbsl) are overlain on the map (contour interval is 15 m).

southern mid-shelf relative to the northern mid-shelf. A saddle between the plunging tip of the Lachlan anticline and the uplifting coast east of Poverty Bay separates the mid-shelf depocenters. The northern depocenter thins through Poverty Gap but thickens again as it connects to the outer shelf depocenter. Dashed extensions (Fig. 5) on the southern syncline axis denote our inference of structural continuity between the basin, Mahia syncline (Berryman, 1993a,b), and subsidence beneath Poverty Bay Flats (Brown, 1995). Evidence of tectonic tilting in well logs beneath Poverty Flats (see Wolinsky et al., this issue) and uplifted shoreline terraces above the northern coast of Mahia Peninsula (Fig. 5) reveals the onshore extension of deformation.

Maximum sediment thickness in the southern depocenter (~70 m) is considerably higher than on the northern (~45 m) and outer shelf (~55 m). It is worth noting here that the southern isopach is appreciably thicker than that mapped by Foster and Carter (1997) and Orpin et al. (2006). The disagreement is due to the fact that they traced W1 into the southern depocenter on a horizon in the 3.5 kHz profiles that corresponds to what we interpret as a shallower, Holocene reflector in our chirp records.

4.2. Post-W1 chronostratigraphy: core-seismic integration

In this section we integrate three giant piston cores – two recovered from the mid-shelf depocenters and a third from the outer shelf – with the chirp data to establish a chronostratigraphy for the post-glacial sediment record on the Waipaoa shelf (Figs. 7–9). Our age model is based primarily on the identification of three geochemically distinct tephras. The ashes were ejected during volcanic eruptions in the North Island's Taupo Volcanic Zone (TVZ). Ages for the tephras have been established from widely observed terrestrial deposits (see Alloway et al., 2007, for dates reported here and additional background on NZ tephrochronology). We interpret the ash beds as primary airfall tephras that settled through the water column, deposited, and in some cases were reworked. Supporting this view are corrected ^{14}C dates from shells above and below the tephras in each of the cores. Though not presented here (see Alexander et al., manuscript in preparation), the dates are consistent with ages for the tephras based on their terrestrial occurrence. The three tephras conveniently subdivide the early eustatic highstand period (~5500 cal. yr BP to present) into three approximately equal time intervals. To mark the late eustatic rise, we report the depth of the Pleistocene–Holocene boundary (~10000 cal. yr BP) in each core predicted by the ^{14}C age model.

To link the tephra and ^{14}C markers in core (depth) with mappable seismic horizons in the chirp profiles (two-way travel time), we use MST logs to establish time-depth relationships for the core intervals at each site. Results for the two mid-shelf cores are summarized in Fig. 8A and B, where physical property logs for MD3004 (southern depocenter) and MD3007 (northern depocenter) are shown. Included in each log panel is the synthetic seismic trace predicted from the core impedance log that was used to tie core depths to the seismic two-way travel times. Each synthetic trace is overlain on the seismic data (Fig. 7B and D). Both synthetic traces are stretched in two-way travel time to produce the best possible match to the field records. In other words, the two-way travel times predicted from measured (MST) p-wave velocities and core depths appear to underestimate the actual two-way travel times over the cored interval. There are two potential sources for the discrepancy: (1) anomalously high p-wave measurements on the cores, or (2) shortening of the piston cores during extraction that caused measured thickness to be less than in situ thickness. Since the measured p-wave velocities are not

Please cite this article as: Gerber, T.P., et al., The influence of sea level and tectonics on Late Pleistocene through Holocene sediment storage along the high-sediment supply Waip..., Mar. Geol. (2009), doi:10.1016/j.margeo.2009.10.002

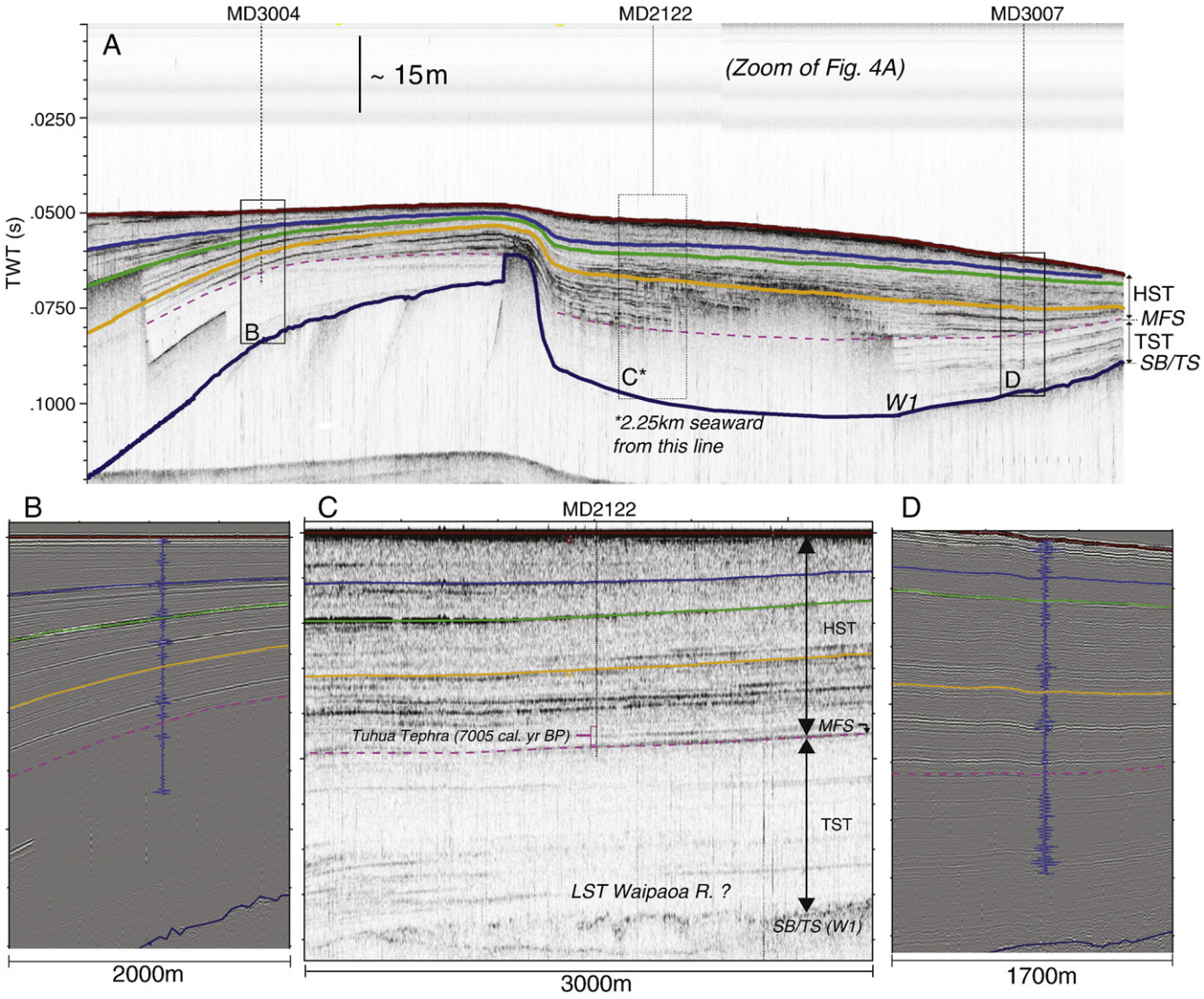

Fig. 7. A) Interpreted middle segment of seismic strike line shown in Fig. 4A. Marker horizons are discussed in text and defined in the log panels of Fig. 8. Core sites MD3004 and MD3007 are also shown; boxes enclose traces shown in parts B and D. The MD2122 core site lies 2.25 km seaward from this line (shown in part C), so its projection is shown here. B) Synthetic chirp trace overlain on trace amplitudes recorded at the MD3004 core site. Synthetic trace produced using the physical property logs in Fig. 8A. C) Chirp seismic trace envelopes crossing the site of core MD2122 (see Gomez et al., 2004). Tephra marker horizons mapped across the site are shown along with the inferred depth of the Tuhua marker, which was not sampled in the MD06 cores. Terminology for the sequence-stratigraphic interpretation follows Fig. 1. D) Synthetic chirp trace overlain on trace amplitudes recorded at the MD3007 core site. Synthetic trace produced using the physical property logs in Fig. 8B.

unreasonable for fine, unconsolidated marine muds (Hamilton, 1971), we believe the latter effect is dominant. Assuming this, an average shortening of 6.5% and 7.1% of the in situ thickness for MD3004 and MD3007, respectively, can account for the mismatch we identify.

A similar correlation plot for the outer shelf core (MD3006) is shown in Fig. 9. The synthetic trace for this core is also adjusted to provide satisfactory agreement with the chirp data, but in this case a match required both stretching and compression in two-way travel time. Again assuming measured (MST) p-wave velocities are accurate, an average lengthening of 3.3% of the in situ thickness accounts for the mismatch. We note that a similar analysis reported by Széréméta et al. (2004) showed both types of sampling anomaly seen in other giant piston cores collected aboard the R/V *Marion Dufresne*. As in their study, neither stretching nor compression anomalies were obvious from visual inspection of the cores. The issue concerns us only insofar as it must be accounted for in our core-to-core correlation and sediment isopaching.

Accepting this, we highlight our tephra-bound chronology for the mid- and outer shelf in Figs. 7–9. The most prominent ash bed in all three cores is identified with the Waimihia eruption (Waimihia tephra; 3410 cal. yr BP) from the Taupo caldera (TVZ). This tephra, widely recognized in terrestrial and marine records around the North Island, is 15–20 cm thick in MD3004 and MD3006 (Fig. 10A–B) but less well-preserved in MD3007 (Fig. 10C). Another, younger tephra (Taupo tephra; 1718 cal. yr BP) widely sampled and correlated across North Island terrestrial and marine records is preserved in MD3006, but apparent bioturbation in mid-shelf cores makes its visual identification difficult. For this reason, the Taupo tephra marker is tied in MD3004 and MD3007 to the base of peaks in magnetic susceptibility that we interpret as the primary occurrence of the tephra. Recovery and identification of Taupo tephra at 2.3 m depth in MD3001 – collected just adjacent to MD3007 – corroborate this interpretation, as do ^{14}C dates in each of the cores. Both the Waimihia and Taupo tephra horizons coincide with reflectors that can be traced between and beyond MD3004 and MD3007 (Fig. 7A), but the corresponding reflectors on the outer shelf (Fig. 9A) tied to the same marker horizons in MD3006 cannot be traced through Poverty Gap.

Please cite this article as: Gerber, T.P., et al., The influence of sea level and tectonics on Late Pleistocene through Holocene sediment storage along the high-sediment supply Waip..., Mar. Geol. (2009), doi:10.1016/j.margeo.2009.10.002

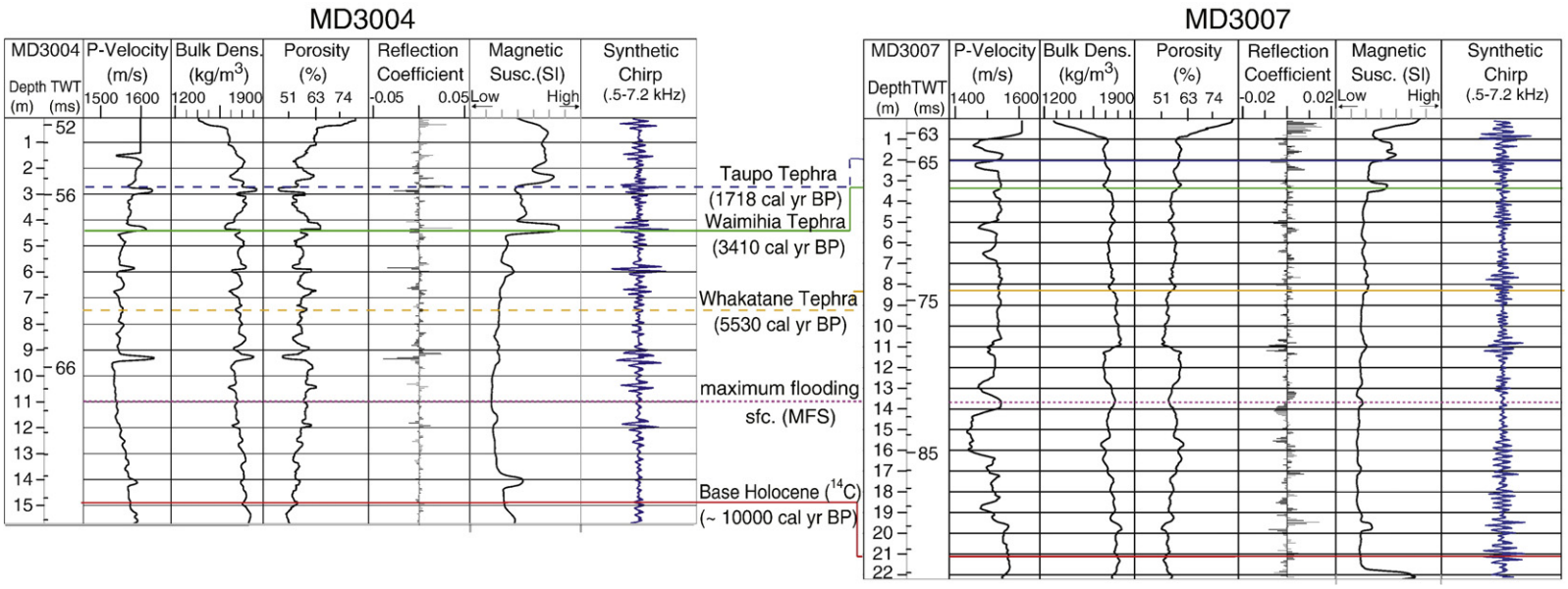

Fig. 8. Physical property logs for piston cores MD3004 (left) and MD3007 (right). Time-depth relationship (far left panels) is adjusted based on comparison of synthetic trace (far right panels) to chirp data in Fig. 7B,D. Tephra horizons sampled and identified in core are indicated with a solid line; those inferred from correlation and/or the ^{14}C chronology of Alexander et al. (manuscript in preparation) are marked with a dashed line.

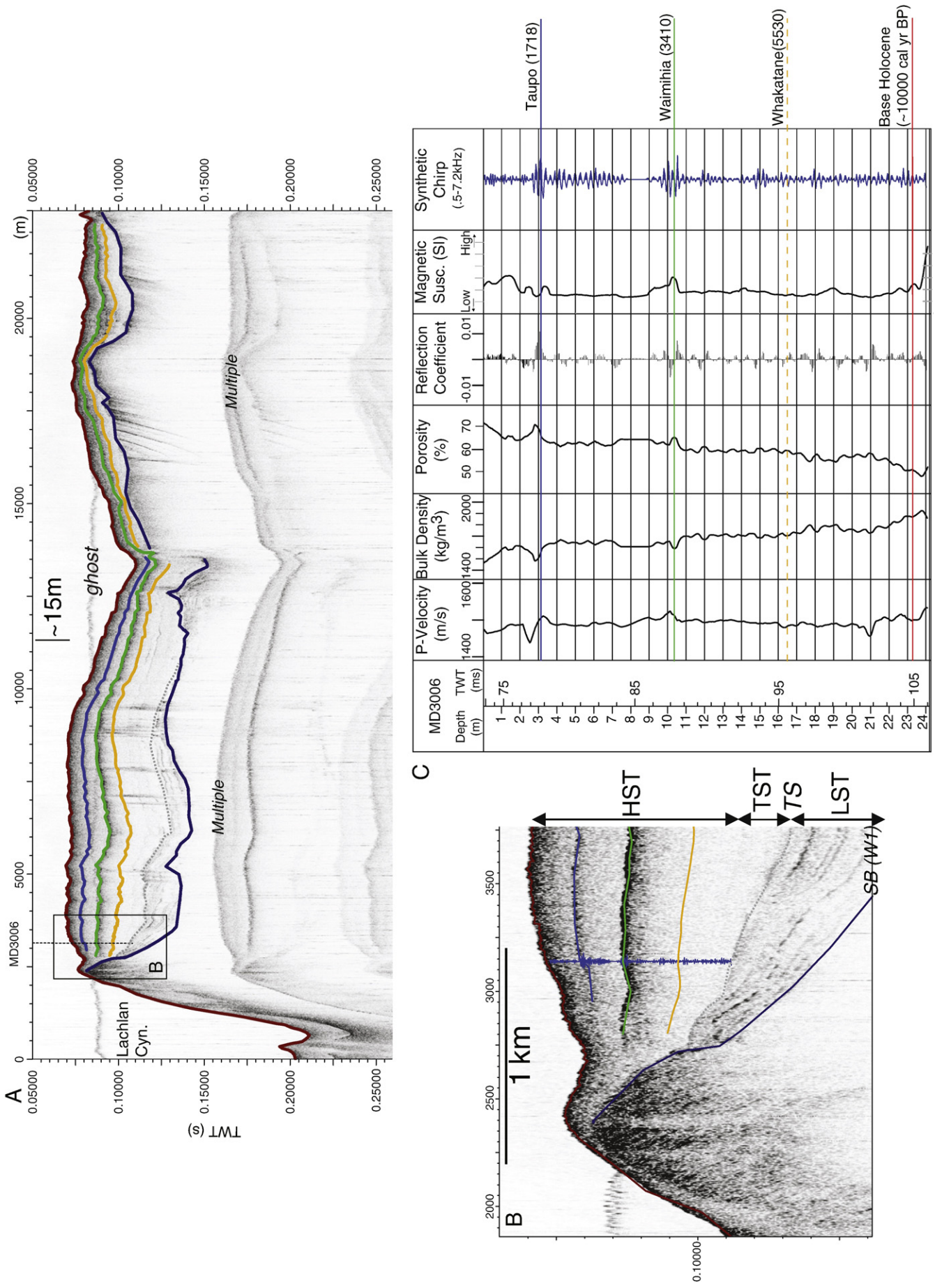

Please cite this article as: Gerber, T.P., et al., The influence of sea level and tectonics on Late Pleistocene through Holocene sediment storage along the high-sediment supply Waip..., Mar. Geol. (2009), doi:10.1016/j.margeo.2009.10.002

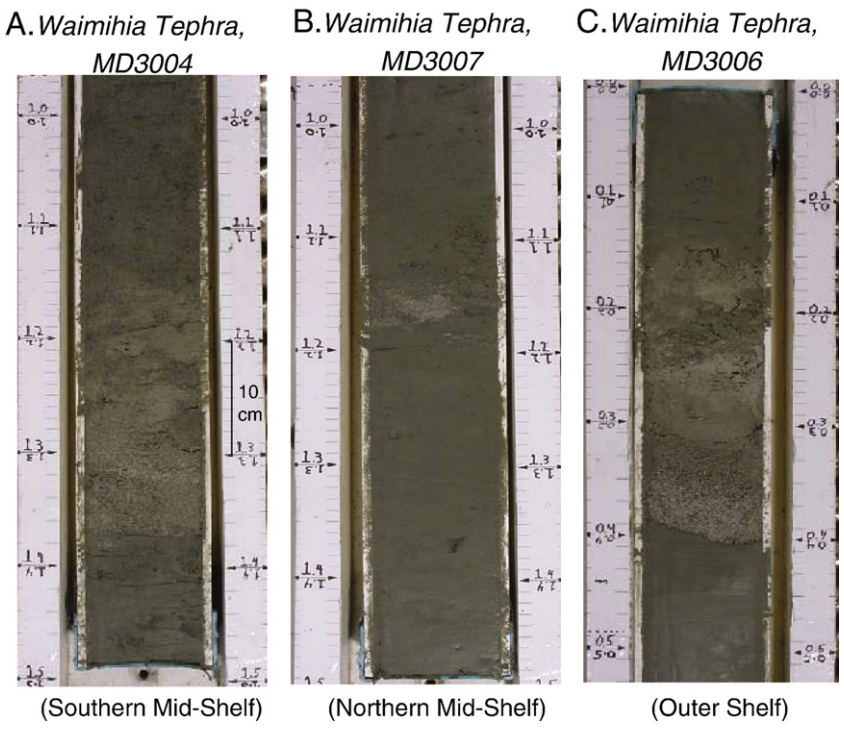

Fig. 10. Example photographs of macroscopic Waimihia tephra recovered in (A) MD3004, (B) MD3007, and (C) MD3006.

A third Holocene tephra in MD3007 is identified with the Whakatane eruption (Whakatane tephra; 5530 cal. yr BP) from the Okataina caldera (TVZ). Like the Taupo tephra it also appears bioturbated in the core, but unlike both of the younger tephras it does not show elevated magnetic susceptibility and has only a modest effect on the impedance log. Whakatane tephra has not been identified in cores MD3004 and MD3006 but both contain shells of similar age. The Whakatane marker horizon is extended away from MD3007 and MD3004 by tracing a semi-continuous reflector across the mid-shelf. Because the seismic character is transparent at the Whakatane depth on the outer shelf, the marker is mapped away from the core by simply paralleling the draped geometry of overlying reflectors.

The Whakatane, Waimihia, and Taupo tephra markers were all identified in a previous core (MD2122) first described by Gomez et al. (2004). The site of this core is covered by the chirp survey and shown in Fig. 7C. The three marker horizons traced away from the MD06 core sites are shown on the plot. Combining two-way travel times for each horizon at the MD2122 site with the core depths for each tephra marker reported by Gomez et al. (2004) implies low apparent velocities, which may also indicate shortening of the piston core upon recovery. As we show in Section 6, our computed mass accumulation rates for the MD2122 site based on the correlation in Fig. 7C are in reasonable agreement with measurements made directly on the core by Gomez et al. (2007). Given this, we forego further inquiry and simply note that the apparent shortening is not inconsistent with our analysis of the MD06 cores. Note on Fig. 7C we have also approximated the location of a fourth tephra marker (Tuhua tephra, 7005 cal. yr BP) identified in MD2122 but not yet sampled in the MD06 cores.

The ^{14}C age model indicates that all three piston cores stopped just below the Pleistocene–Holocene boundary (Figs. 7–9). Thus each core contains a full Holocene record and, importantly, a record of rising eustasy along the New Zealand coastline. In the following section we use this finding to develop our sequence-stratigraphic model for the post-glacial flooding of the Waipaoa shelf.

5. Sequence-stratigraphic interpretation

Together, the W1 surface and the four marker horizons defined above provide a chronostratigraphic framework for interpreting the Late Pleistocene and Holocene evolution of the Waipaoa shelf. In this section we combine that framework with sequence-stratigraphic principles to interpret key surfaces and stratal patterns associated with changes in accommodation during the last glacioeustatic rise and ongoing tectonic deformation. Standard sequence-stratigraphic terminology is used and follows Fig. 1 (see caption).

5.1. Late lowstand and transgressive strata: W1 and the shelf flooding surface

The eustatic sea level fall and subsequent rise that accompanied the last glacial advance and retreat strongly influenced Late Pleistocene and Holocene accommodation on the Waipaoa margin. Global sea level fell 120 m below its present level between ~120,000 and ~20,000 cal. yr BP (Pillans et al., 1998; Fig. 11A). Eustatic sea level subsequently rose with deglaciation, reaching its present level along the coast of New Zealand around 7000 cal. yr BP (Gibb, 1986; Fig. 11B). The rapid increase in accommodation during this period forced a

Fig. 9. A) Interpreted middle segment of seismic strike line shown in Fig. 4C. Marker horizons are discussed in text and defined in Part C. Core site MD3006 is also shown; box encloses traces shown in Part B. B) Synthetic chirp trace overlain on trace envelopes recorded at the MD3006 core site. Terminology for sequence-stratigraphic interpretation follows Fig. 7. C) Physical property logs for piston core MD3006. Time-depth relationship (far left panel) is adjusted based on comparison of synthetic trace (far right panel) to chirp data in Part B. Tephra horizons sampled and identified in core are indicated with a solid line; those inferred from correlation and/or the ^{14}C chronology of Alexander et al. (manuscript in preparation) are marked with a dashed line.

Please cite this article as: Gerber, T.P., et al., The influence of sea level and tectonics on Late Pleistocene through Holocene sediment storage along the high-sediment supply Waip..., Mar. Geol. (2009), doi:10.1016/j.margeo.2009.10.002

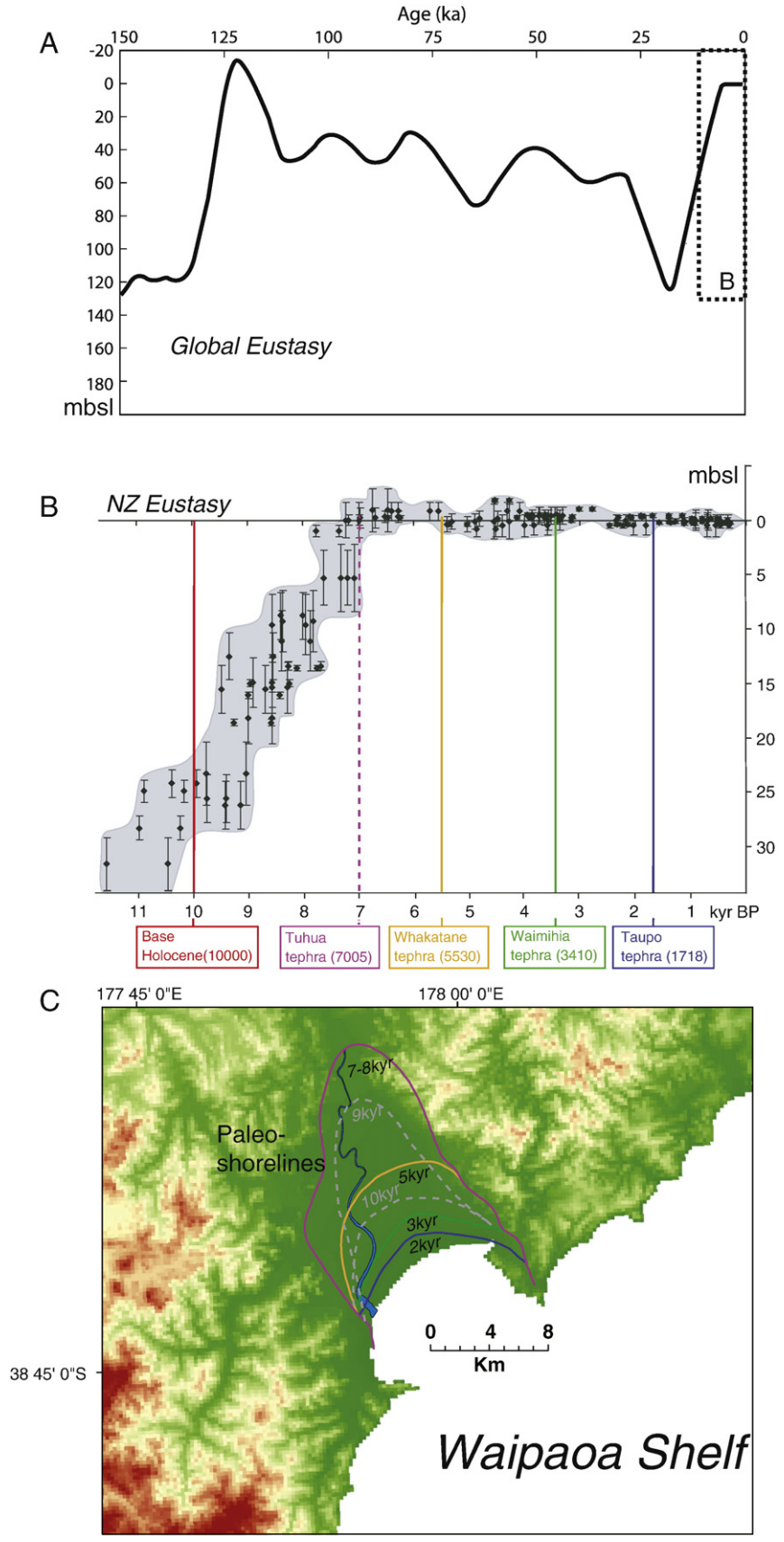

Fig. 11. A) Representative global eustatic curve following Pillans et al. (1998) and Slingerland et al. (2007) with approximate age range for Late Pleistocene tephras recovered in MD3004 and MD3007 included. B) Holocene eustatic curve for New Zealand based on Gibb's reconstruction (1986) and reproduced from Cochran et al. (2006). Included are ages of Holocene tephras discussed in text. C) Mapped paleo-shorelines beneath Poverty Flats from Brown (1995).

Please cite this article as: Gerber, T.P., et al., The influence of sea level and tectonics on Late Pleistocene through Holocene sediment storage along the high-sediment supply Waip..., Mar. Geol. (2009), doi:10.1016/j.margeo.2009.10.002

shoreline transgression across the margin, the latter stages of which are recorded landward of the shelf by paleo-shorelines beneath the modern coastal plain of the Waipaoa River (Poverty Flats, Fig. 11C).

We interpret the W1 unconformity as a sequence boundary (SB) associated with the last sea level fall and consequent shoreline regression. Where visible on the mid-shelf, W1 cuts into a deformed, consolidated substrate and is traceable onto the exposed cores of the anticlines (Fig. 4A; Fig. 7). None of the piston cores penetrated the buried extension of W1, but where exposed on the uplifted northern flank of the Lachlan structure the surface was mantled with gravels interpreted as lowstand deposits of the Waipaoa River (Wood, 2006). In places, diffuse reflections on W1 may indicate the presence of thin lowstand gravels (Fig. 7C), but the chirp records show no prominent incised valley, suggesting limited fluvial incision into the exposed shelf as the shoreline moved seaward.

On the outer shelf, W1 defines a wave-planed terrace on the seaward flank of the Ariel anticline that we interpret to be the last lowstand shoreline (Fig. 12A–B). A strong angular unconformity draped with post-glacial mud (transparent acoustic facies) delineates the terrace, which extends parallel to the anticline's crest and the modern coastline. W1 shows similar character along most of the outer shelf except where it extends beneath the depocenter lying just north of Lachlan canyon (Fig. 4C; Fig. 9), where the sequence boundary underlies a package of parallel and truncated reflectors that thicken towards the canyon head. There, W1 diverges from a separate unconformity that marks the boundary between the truncated unit and the overlying transparent seismic facies (gray dashed line in Fig. 9A–B).

Two primary seismic facies are above W1 near MD3004 and MD3007 (Figs. 4A; 7A,C). An acoustically transparent facies with a few weak, discontinuous reflectors characterizes the older unit, which is overlain by a highly reflective package containing multiple continuous reflectors. The facies break corresponds to a downlap surface for the oldest reflectors in the overlying unit. In the cores, the break corresponds to a depth 5–7 m above the Pleistocene–Holocene boundary. At site MD2122, the break is near the inferred travel-time depth for the Tuhua tephra (~7000 cal. yr BP).

Unlike the mid-shelf, no distinct acoustic facies break divides the outer shelf depocenter above W1 except for the unit adjacent to Lachlan canyon (Fig. 9). The MD3006 core stopped in this unit, and visual descriptions of the core indicate sands in its base. The ^{14}C age model for MD3006 indicates the contact is at or near the Pleistocene–Holocene boundary.

Taken together, the seismic and core evidence support the following sequence-stratigraphic interpretation. The mid-shelf facies boundary described above is a maximum flooding surface (MFS) that formed as the transgressing Waipaoa shoreline reached its maximum inland extent. As seen in Fig. 11C, the age of the most landward paleo-shoreline mapped in Poverty Bay matches that estimated for the culmination of eustatic sea level rise (~7000 cal. yr BP) and the Tuhua tephra marker identified in MD2122, which lies at or near our placement of the MFS (Fig. 7). The seismic downlap of overlying reflectors – a diagnostic attribute of shelf flooding surfaces – marks the onset of coastal progradation in Poverty Bay and highstand sediment delivery to the shelf. The latter is further evidenced by a coarsening upward trend seen in grain size measurements from MD2122 above our placement of the MFS (Gomez et al., 2004). On the outer shelf the MFS is not resolvable, but we infer its presence within the 5–6 m condensed section (i.e., an interval of low accumulation rates) between the base of the core and the Whakatane marker horizon (Fig. 9).

Extending our sequence-stratigraphic approach (i.e., Fig. 1), we expect a mid-shelf succession below the MFS and above W1 consisting of late lowstand to early transgressive paralic strata capped by a transgressive wave ravinement surface (TS) and overlain by a condensed section of late transgressive and early highstand strata. On the outer shelf near the lowstand shoreline, we expect to observe a ravinement surface cutting either lowstand deltaic deposits or the sequence boundary (W1) and capped by thin, hemipelagic drape. The truncated outer shelf unit adjacent to Lachlan canyon may in fact be a deltaic unit associated with the lowstand Waipaoa (Fig. 9), and where W1 is overlain directly by thin transparent facies there is neither a well-developed transgressive surface nor overlying transgressive deposits (e.g., Fig. 12B).

Characterizing facies beneath the MFS in the mid-shelf depocenters is more difficult, especially given the lack of detailed textural and paleoenvironmental indicators. The interval lying between the MFS and W1 is approximately 15 m thick near the core sites and even

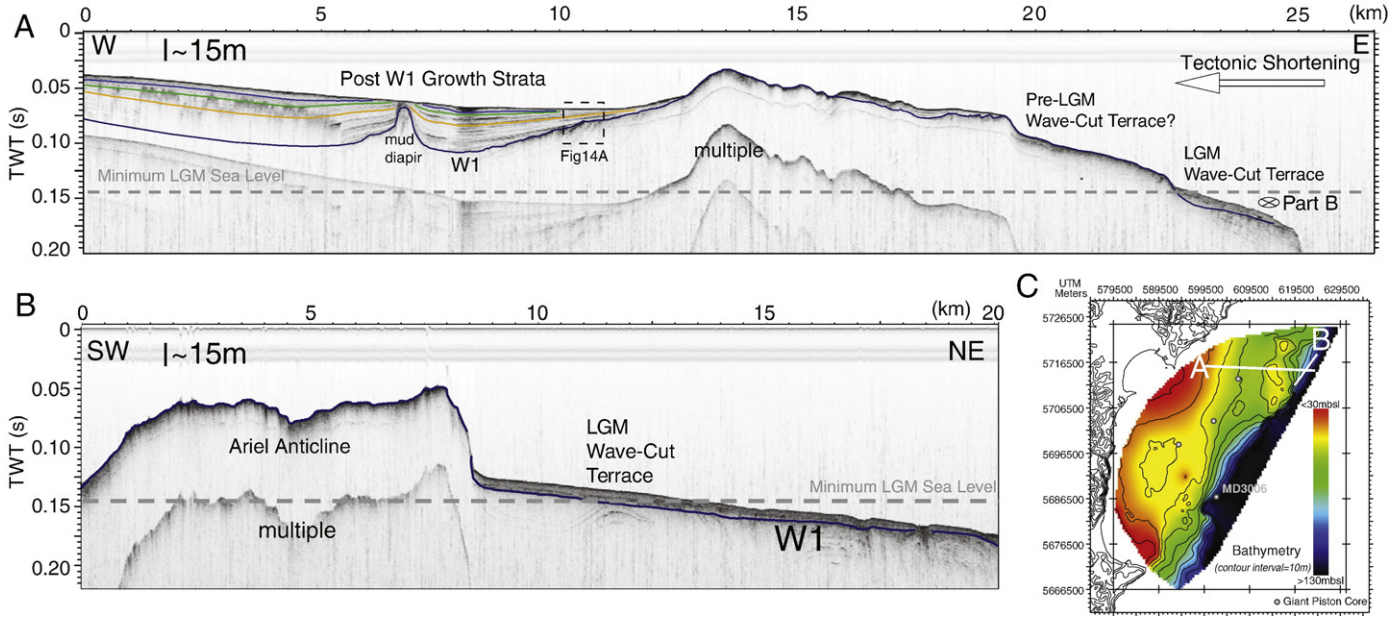

Fig. 12. A) Shore-perpendicular seismic line across the northern subbasin and the Ariel anticline. Labels in this figure and Part B refer to discussion in text, and vertical scale in each panel is two-way travel time with approximate depth scale in meters assuming a sound velocity of 1500 m s^{-1}. Intersection with line in Part B is marked. B) Shore-parallel line along outer shelf seaward of Ariel anticline. Location of both lines is indicated on the bathymetric map in Part C. Note that projection of LGM sea level in Parts A and B includes correction for the depth of the Chirp hydrophones in TWT.

Please cite this article as: Gerber, T.P., et al., The influence of sea level and tectonics on Late Pleistocene through Holocene sediment storage along the high-sediment supply Waip..., Mar. Geol. (2009), doi:10.1016/j.margeo.2009.10.002

thicker in the basin deeps. Foster and Carter (1997) and Orpin et al. (2006) interpreted W1 as the TS, which implies that the interval below the base of the mid-shelf cores was deposited seaward of a transgressing shoreline prior to ~10000 cal. yr BP. This is consistent with the lack of a mappable seismic discontinuity above W1 that would indicate a separate overlying TS. Together, their interpretation and previous estimates for the marine incursion of Poverty Bay (10,000–11,000 cal. yr BP, Fig. 10C; Brown, 1995) suggest a relatively thick, well-preserved transgressive unit on the Waipaoa mid-shelf.

Given this, we interpret the TS to lie directly on the SB (W1) across most of the Waipaoa shelf. Evidence for Late Pleistocene lowstand deposits appears to be largely absent, except for the outer shelf unit noted above (Fig. 9) and a package directly overlying W1 landward of Ariel anticline (Figs. 12A; 14A). Without additional evidence from the deposits beneath the cored interval we are unable to develop the model further. At present, it is unclear when – in terms of eustasy and the position of the paleo-shoreline – erosion on W1 ceased and sediments began accumulating, and whether the deposits are primarily nearshore, estuarine, or inner-shelf facies is not addressed here.

Nevertheless, it is worth remembering that like most sequence boundaries, W1 is a diachronous surface formed during shoreline migration. Where imaged clearly, W1 apparently cuts not into shelf sediments of the previous highstand but older, deformed rocks of the accretionary prism. This suggests that in addition to recording transgressive wave ravinement during the last eustatic rise W1 may also bear the signature of multiple sea level lowstands. Implicit in this view is that previous sequences of lowstand, transgressive, and highstand deposits may be confined to the gas-obscured basin deeps. And as we show in Section 5.2 (see also Wood, 2006), W1 also records highstand ravinement where it shoals to depths at or above modern fair-weather wave base on the anticline crests.

In summary, seismic and core data support the identification of a flooding surface (MFS) across the Waipaoa shelf that is of similar age to the most landward mapped shoreline in Poverty Bay and regional estimates for the culmination of the post-glacial eustatic rise. If the transgressive surface (TS) lies directly on the sequence boundary (W1) across most of the mid-shelf, then a relatively thick transgressive unit is preserved but few lowstand deposits. In this case, strata directly overlying W1 in the subsiding shelf basins formed during the end of falling or minimum eustasy (as in the generic sequence in Fig. 1). More detailed sedimentological data should resolve the nature of deposition immediately beneath the MFS.

5.2. The modern highstand: tectonic controls on accommodation

In this section we consider in more detail highstand strata above the MFS. In the present eustatic stillstand that began 7000 cal. yr BP, the dominant control on highstand accommodation is the ongoing tectonic deformation across the shelf. In Section 4.1 we contrasted stratal geometry and character between the two mid-shelf (Fig. 4A) and outer shelf (Fig. 4C) subbasins, noting differences across the mid-shelf that are even expressed in the seafloor bathymetry (Fig. 4D). Reflectors in the southern depocenter define an underfilled syncline, where the subsidence pattern evident in the post-W1 isopach is mirrored at the seafloor. In contrast, the stratal geometry of the northern depocenter shows a more progradational pattern along strike, and the highstand prism resembles a low gradient clinoform in dip profile (Fig. 12A). Spatial and temporal variation in the mid-shelf subsidence pattern can give rise to such differences, but mapping out the detailed structural evolution of the shelf is beyond the limits of the shallow chirp and core data presented here. Yet a closer look at stratal patterns in the early highstand growth strata provides clues to the ongoing tectonic modulation of shelf infilling.

We infer the uplift and subsidence history of the Lachlan anticline and southern syncline, respectively, from the termination patterns of highstand marker horizons along the Lachlan structure. A series of chirp transects in Fig. 13 covering the transition from syncline to anticline flank shows a systematic pattern moving south to north along the crest of the structure. The southernmost line, just offshore from Mahia Peninsula, shows an upturned package of post-W1 strata with apparent truncation of the oldest highstand marker horizons (Fig. 13E). Moving north, apparent truncation of the growth strata gives way to seismic offlap with an increasing degree of seismic pinch-out (Fig. 13D–C). Further north, the same unit progressively onlaps onto the uplifting anticline (Fig. 13B) and, at the northernmost crossing, is seen to completely drape the tip of the structure (Fig. 13A). Note the depth of the anticline crest varies little between transects.

If wave and current reworking of the seabed depend primarily on water depth, then the preservation potential for sediments deposited across a growing fold should depend on its uplift history during basin filling. We therefore interpret the pattern seen in Fig. 13A–E to result from a decrease in uplift relative to sediment accumulation from south to north along the Lachlan structure that probably reflects its northward propagation into the Waipaoa margin (Fig. 13G). Where uplift is greatest in the south – that is, from high rates of uplift sustained for longer – early highstand growth strata have shoaled to depths where wave and current reworking (i.e., ravinement) can occur (Fig. 13E). Where uplift is reduced in the north, highstand marker horizons define a growth package that tapers toward the fold crest and shows an increasing degree of onlap to the north, suggesting an increase in sedimentation rates relative to uplift (Fig. 13C–B). At the propagating tip of the fold, sedimentation still exceeds uplift and completely buries the emerging structure and the W1 surface. In a general sense, our model for the spatial gradient in stratal geometry along the Lachlan structure (i.e., Fig. 13G) can be thought to approximate the time-evolution along any given transect as the fold propagates northward.

Seismic transects crossing the Ariel anticline do not show a strong margin-parallel gradient in uplift. Yet variations in onlap–offlap geometry in the growth strata along a single transect suggest temporal variation in the accommodation–supply balance across the evolving northern basin (Figs. 12; 14). Early highstand strata onlap onto the emergent Ariel fold, but the termination pattern reverses above the Whakatane marker horizon such that the youngest unit, containing the Waimihia and Taupo markers, shows slight seismic offlap. Evidently, sediments began filling new accommodation during the early highstand period, marked by onlap of the anticline flank coincident with downlap in subsiding shelf reaches. With sea level stabilized, filling of this space and continued uplift on the anticline has limited overall storage in the basin and caused distal strata to offlap the flank. In other words, accommodation in the northern basin may now be filled, with progradation limited by the emergence of the outer shelf. Implicit in this view is that sediments delivered to the northern mid-shelf have increasingly been stored elsewhere, perhaps on the outer shelf, an idea we consider further in the following section.

6. Holocene highstand sediment budget

In this section we quantify the early highstand sediment budget to further evaluate the accommodation–supply balance in each shelf subbasin and constrain the shelf-wide storage of terrestrial sediment. The budget (5530 cal. yr BP to present) is summarized in Figs. 15 and 16. In Fig. 15A–C, we plot three maps showing the spatial variation in

Fig. 13. (A–E). Series of seismic transects crossing the landward flank of Lachlan anticline along the boundary of the southern mid-shelf subbasin. Vertical scale is two-way travel time; an approximate depth scale in meters is shown assuming a sound velocity of 1500 m s^{-1}. Locations of lines are shown on the small bathymetric map in Part F. G) Concept sketch explaining the pattern of stratal termination patterns along the landward flank of Lachlan anticline.

Please cite this article as: Gerber, T.P., et al., The influence of sea level and tectonics on Late Pleistocene through Holocene sediment storage along the high-sediment supply Waip..., Mar. Geol. (2009), doi:10.1016/j.margeo.2009.10.002

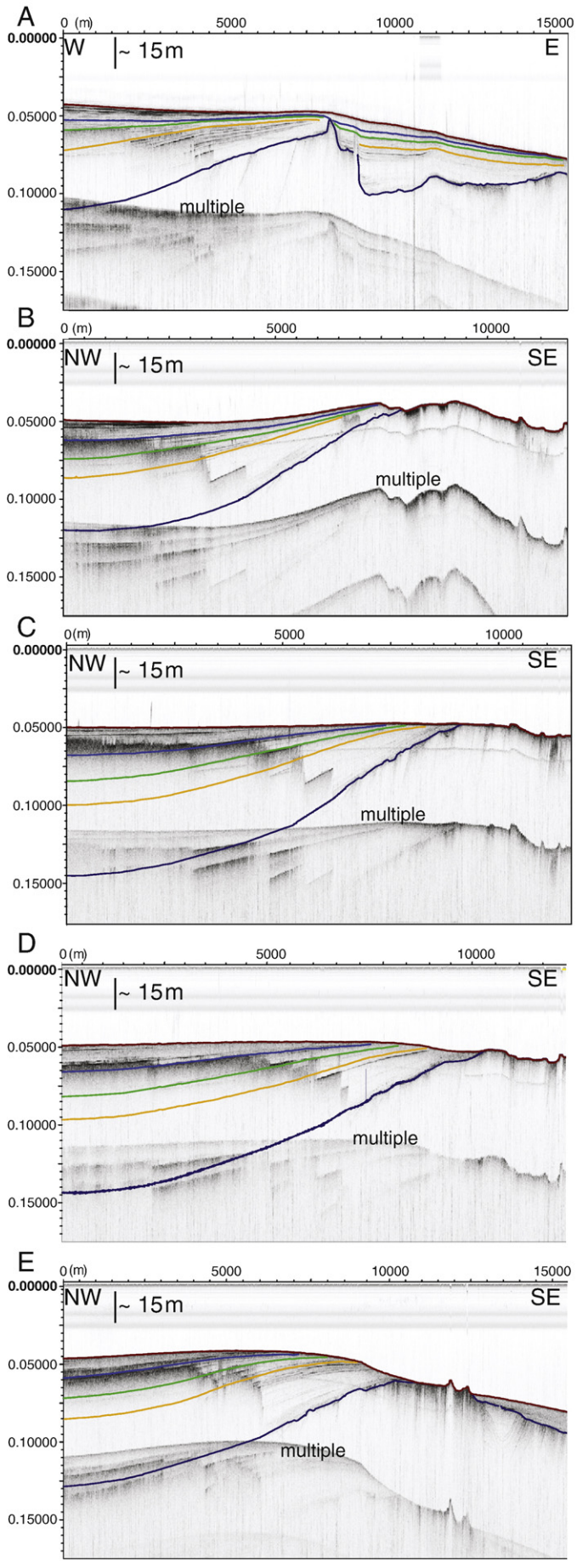

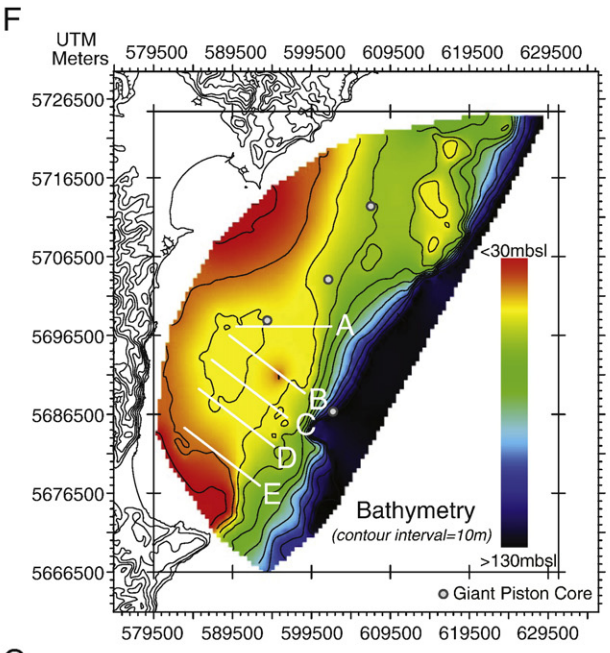

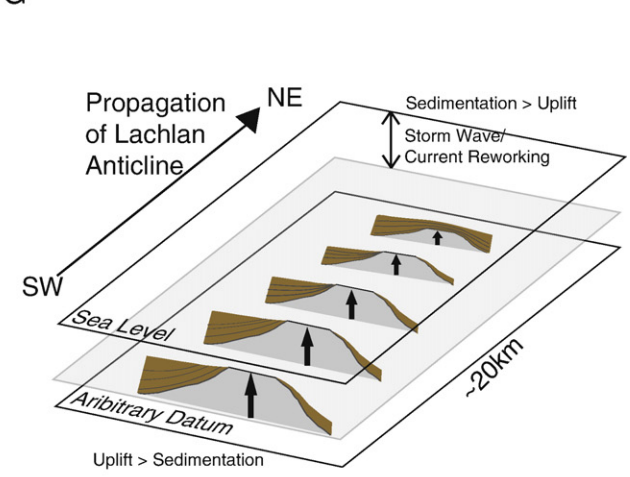

Please cite this article as: Gerber, T.P., et al., The influence of sea level and tectonics on Late Pleistocene through Holocene sediment storage along the high-sediment supply Waip..., Mar. Geol. (2009), doi:10.1016/j.margeo.2009.10.002

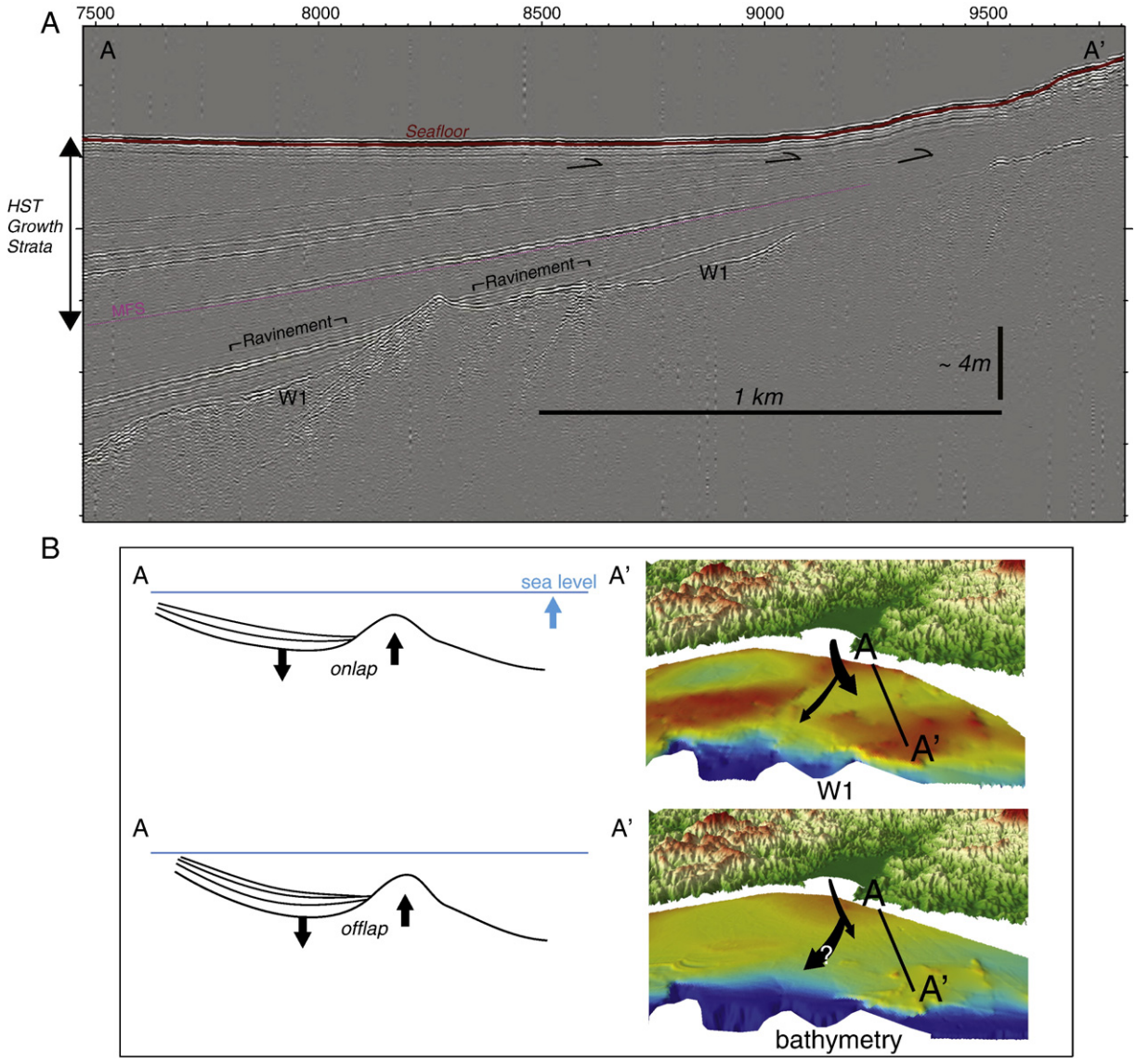

Fig. 14. A) Close up of seismic amplitudes from Fig. 12A where strata pinch-out on the flank of Ariel anticline. B) Concept sketch depicting filling of northern subbasin. Perspective maps of bathymetry (from Fig. 3) and W1 (from Fig. 5) look east towards the Waipaoa River mouth (both in mbsl).

average mass accumulation rate (MAR, $g\,cm^{-2}\,yr^{-1}$) between each interval bounded by the three highstand marker horizons introduced in Section 4.2. In Fig. 16A and B, we plot the total average storage rate ($Mt\,yr^{-1}$) and relative average storage rate (% of total shelf storage) for each interval in the three main shelf depocenters outlined in Section 4.1 and evident in the accumulation rate maps. In Fig. 16C, the total average storage rate ($Mt\,yr^{-1}$) for the entire shelf is plotted with three additional estimates for comparison: (1) the mean and range of suspended sediment loads delivered to Poverty Bay by the Waipaoa River from 3000 to 700 cal. yr BP estimated by Kettner et al. (2007), (2) the modern (gauged) annual suspended sediment output to Poverty Bay (Hicks et al., 1999), and (3) an estimate for the total annual rate of accumulation based on ^{210}Pb chronology (last ~100 yr) reported by Miller and Kuehl (this volume). Finally, the inset to Fig. 16C compares our estimated mass accumulation rates at the MD2122 site (i.e., Fig. 15B–C) to the core-derived estimates reported by Gomez et al. (2007).

6.1. Spatial and temporal trends in highstand shelf accumulation

Several features of our highstand sediment budget stand out. Overall, total shelf storage declines slightly from the mid-Holocene to the present. The difference is small and may not be significant given the uncertainties in our summation. If real, the result suggests either a small increase in sediment export from the shelf and/or a small decline in the supply of sediment to the shelf. But a more important result emerges when our loads are compared to the estimates of Kettner et al. (2007). Their running mean ($=2.3\,Mt\,yr^{-1}$) for the late Holocene prior to human settlement (~700 cal. yr BP) compares favorably to our budget, suggesting that our storage estimates account for most or all of the suspended sediment delivered by the Waipaoa River to the coast during most of the early highstand period. In other words, our best estimate suggests a high shelf trapping efficiency for terrestrial sediment during this period.

The MAR maps and depocenter budget numbers quantify the partitioning of the Waipaoa's highstand load into distinct subbasins. The southern mid-shelf basin is the primary depocenter, containing 60–65% of the total highstand load. The small Holocene decline there is thus the dominant influence on the trend noted above for the total shelf. Storage on the outer shelf is much smaller but also shows a slight Holocene decline. Storage in the northern mid-shelf is more variable, dropping nearly 50% between the oldest two intervals to an average load less than that of the outer shelf. Storage then increases

Please cite this article as: Gerber, T.P., et al., The influence of sea level and tectonics on Late Pleistocene through Holocene sediment storage along the high-sediment supply Waip..., Mar. Geol. (2009), doi:10.1016/j.margeo.2009.10.002

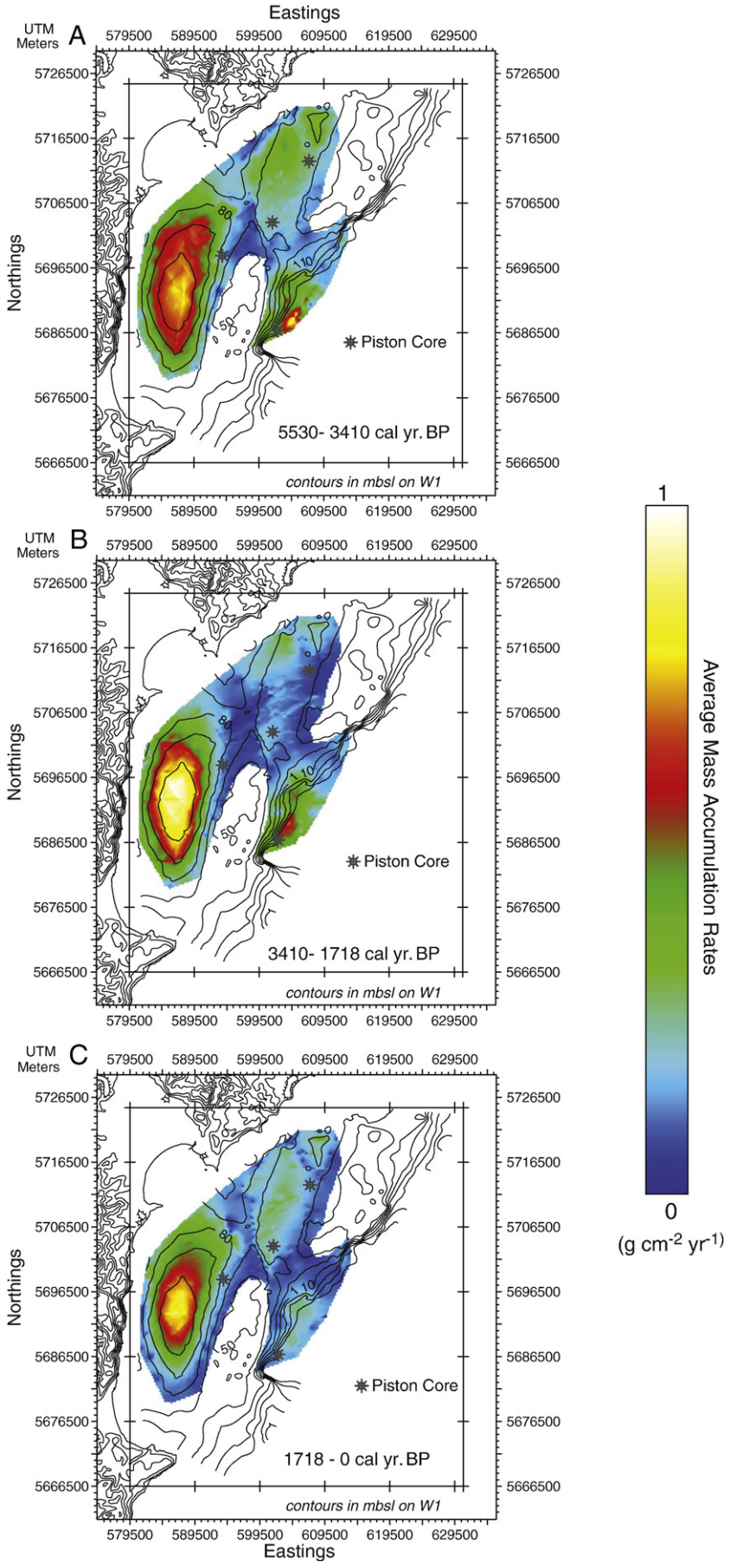

Fig. 15. (A–C) Mass accumulation rate maps for cored intervals bounded by the highstand tephra markers discussed in the text. Contours (15 m interval) are on W1.

Please cite this article as: Gerber, T.P., et al., The influence of sea level and tectonics on Late Pleistocene through Holocene sediment storage along the high-sediment supply Waip..., Mar. Geol. (2009), doi:10.1016/j.margeo.2009.10.002

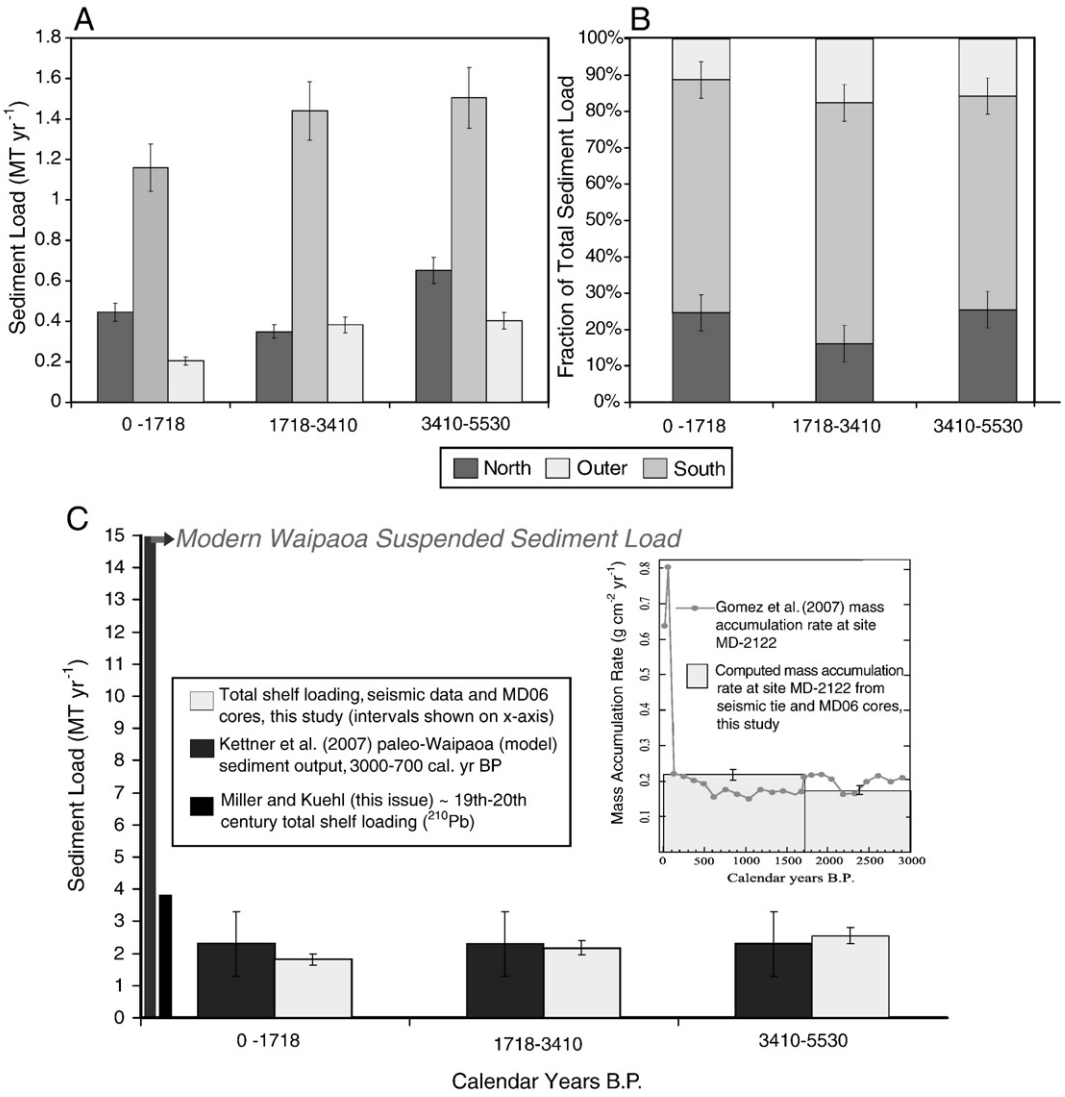

Fig. 16. A) Total load ($Mt\,yr^{-1}$) averaged over the three time intervals shown in Fig. 13 for each shelf depocenter. A constant, ±10% uncertainty is assigned to the load estimates. B) Same as Part A, but now loads are expressed as a fraction of the total shelf storage (from Part C) for each time interval. C) Total shelf loads for each time interval, expressed again with a ±10% uncertainty. Also shown are: the mean (2.3 $Mt\,yr^{-1}$) and range (shown as error bars) of Kettner et al.'s predictions for suspended sediment output from 3000 to 700 cal. yr BP, the 19th–20th century loads estimated by Miller and Kuehl in this volume (3.75 $Mt\,yr^{-1}$), and the modern (gauged) suspended sediment discharge at the coast. (Inset) Mass accumulation rates estimated at the MD2122 site from our seismic mapping and extrapolation of MD06 piston core data. Our average MARs for the two most recent intervals (Fig. 13B–C) are compared with the higher resolution MARs measured directly on the core by Gomez et al. (2007).

by a smaller amount in the most recent interval. Note in the plot of relative depocenter loads that the large decrease in northern mid-shelf storage is accompanied by an increase in the percentage of total storage within the southern mid-shelf and outer shelf basins.

Together with our findings from Section 5.2, the maps and cumulative sediment budget for the Waipaoa shelf support a characterization of the shelf depocenters in terms of the supply–accommodation balance. The underfilled geometry of the southern mid-shelf basin and its large fraction of total sediment storage through the early highstand suggest accommodation-dominated conditions, an idea first put forward by Orpin et al. (2006). In this view, long-term sediment supply is less than the accommodation produced by tectonic subsidence and thus sediment storage is high. Conversely, the stratal geometry observed in the northern mid-shelf basin in combination with the large reduction in sediment storage there suggests supply-dominated conditions. In this view, accommodation produced by tectonic subsidence is less than long-term sediment supply and thus limits sediment storage. A shift to overfilled conditions during the highstand limited storage of sediment delivered to the northern mid-shelf, which may instead have partially bypassed to the outer shelf basin (i.e., Fig. 14B), increasing its fraction of the total shelf load even as absolute accumulation rates declined slightly. The smaller increase in northern mid-shelf storage during the most recent interval may reflect a strong modern supply signal, consistent with the large recent increase in mass accumulation rates estimated from the MD2122 core.

6.2. The anthropogenic supply signal

Not seen in our total shelf sediment budget is the roughly 6-fold increase in sediment discharged by the Waipaoa River that began around 700 yr ago with human settlement and has accelerated over the past two centuries. If the shelf were trapping this elevated fluvial supply, our average load for the most recent interval would not show the modern river output but rather a weighted average that includes the pre-anthropogenic load. Yet this would still exceed the value we estimate. This appears to be the case at the MD2122 core site, where our interval-averaged (i.e., 1718 yr) mass accumulation rate is in good agreement with that expected from the higher resolution core-based estimate of

Please cite this article as: Gerber, T.P., et al., The influence of sea level and tectonics on Late Pleistocene through Holocene sediment storage along the high-sediment supply Waip..., Mar. Geol. (2009), doi:10.1016/j.margeo.2009.10.002

Gomez et al. (2007) (Fig. 16 inset). Yet our total shelf load shows not even a small discernible increase in the modern interval. The deficit can be explained by the recent (100–200 yr) shelf budget based on radionuclide-derived sedimentation rates, which suggests that only 25% of the current (i.e., 3.75 of 15 $Mt\,yr^{-1}$) Waipaoa load is retained on the shelf (Miller and Kuehl, this volume). In other words, a storage increase to 3.75 $Mt\,yr^{-1}$ instead of 15 $Mt\,yr^{-1}$ over the last few hundred years would be difficult to detect in our ~1700 yr average estimate. We conclude, then, that shelf-wide accommodation largely balanced the pre-anthropogenic supply (high trapping efficiency), but the high anthropogenic supply has tipped the balance and generated significant shelf bypassing and sediment export to the slope (low trapping efficiency).

7. Discussion

7.1. Stratigraphic architecture

Our sequence-stratigraphic interpretation for the shelf suffers from our inability to characterize the late glacioeustatic lowstand in the seismic and core records and determine the extent to which sequences analogous to that shown in Fig. 1 are preserved in the Waipaoa basin deeps. For example, we have not identified W1 cutting regressive shelf strata formed prior to or during the sea level fall. But regardless of long-term preservation potential, development of the modern sequence evidently varies across the tectonically segmented Waipaoa shelf. In general, we conceptualize the relative thickness and stacking of strata deposited during the last eustatic fall and rise along a continuum between well-developed sections in high-subsidence settings to missing sections on uplifting structures where ravinement occurs today (Fig. 17).

We are unable to probe the deeper structure beneath the Waipaoa margin to reveal the displacements driving surface deformation evident in the shallow shelf stratigraphic record. Nevertheless, the uplift we document along the Lachlan anticline (Figs. 5A; 13) is probably coseismic in origin. Large, subduction-related earthquakes are well documented along the extension of Lachlan Ridge south of the Waipaoa margin (Barnes et al., 2002), and uplifted Holocene shoreline terraces along Mahia Peninsula (Fig. 5B) are attributed to five large earthquakes that occurred over the last 5000 yr with a mean recurrence interval of ~1000 yr and vertical displacements ranging from 1 to 4 m (Berryman, 1993a,b). Linked coseismic subsidence for the oldest event is documented for coastal sites within the Mahia syncline to the south (Cochran et al., 2006), and thus may also have affected the southern mid-shelf basin on the Waipaoa margin (Fig. 5A). Evidence for coseismic uplift and subsidence on the Ariel anticline and northern mid-shelf basin, respectively, is sparse, but uplifted Holocene shoreline terraces are also above the northern coast of Poverty Bay and are considered coseismic in origin (Berryman et al., 1989).

In addition to raising marine terraces, coastal uplift along the North Island East Coast elevated a number of estuarine sequences formed during the late eustatic rise, including preserved sections north of Poverty Bay ('Sponge Bay'; Ota et al., 1988) and the northern Mahia coast ('Whangewehi Stream'; Berryman, 1993a,b). These 5–10 m preserved sections are correlative with thicker packages of estuarine sediment buried beneath the subsiding zones of Poverty Flats (Brown, 1995). Importantly, our study provides the first offshore characterization of coeval transgressive sediments, i.e., those mapped between W1 and the MFS. Our analysis provides a framework for interpreting forthcoming textural analyses for the MD06 cores at this depth, and will aid reconstruction of transgressive depositional environments from the shoreline to the shelf edge.

7.2. Holocene sediment budget

Our sediment budget for the eustatic highstand period shows a small decline in accumulation rates across the three averaging intervals (~5500 cal. yr BP to present) that is probably within the range of combined uncertainty for our isopaching and chronology. Nevertheless, the trend may indicate a small increase in sediment export from the shelf during the middle and late Holocene and/or a steadily decreasing supply to the shelf. The former may be explained by evidence for late Holocene infilling in the head of Lachlan canyon (Fig. 9), which we have not mapped for our budget but could be volumetrically significant (Walsh et al., 2007). An explanation for declining sediment supply prior to human settlement is beyond the scope of this paper, but studies of sediment transfer through Poverty Flats and Poverty Bay may shed additional light on the question.

Previous attempts at a post-glacial sediment budget for the Waipaoa shelf by Foster and Carter (1997) and Orpin et al. (2006) also failed to balance long-term shelf storage and the modern, anthropogenically influenced Waipaoa loads, leading them to infer significant modern export of sediment to the slope. We have reached the same conclusion, but have corroborated the claim with more detailed seismic mapping and additional long core data. Most importantly, our findings are cast alongside new estimates for Holocene sediment loads from the Waipaoa River to demonstrate a high trapping efficiency for the shelf prior to anthropogenic disturbance in the catchment. This result is surprising in light of predictions for high off-shelf sediment export from narrow shelves with a high fluvial sediment supply (Walsh and Nittrouer, 2003), and probably reflects the tectonic generation of shelf accommodation. Still, those same predictions imply that the amount of sediment retained on modern shelves is

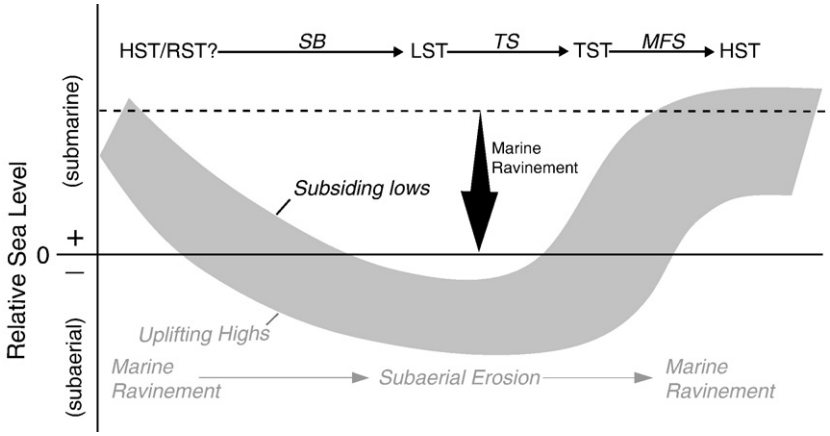

Fig. 17. Simple concept sketch of relative sea level fall and rise along the Waipaoa shelf. Upper and lower edges of dark gray band represent subsiding and uplifting endmembers, respectively. Expected sequence of strata in subsiding shelf depocenters (top) gives way to marine ravinement and subaerial exposure (bottom) on uplifting structures.

Please cite this article as: Gerber, T.P., et al., The influence of sea level and tectonics on Late Pleistocene through Holocene sediment storage along the high-sediment supply Waip..., Mar. Geol. (2009), doi:10.1016/j.margeo.2009.10.002

sensitive to sediment supply, as our Waipaoa budget and the recent storage estimates of Miller and Kuehl (this volume) suggest.

8. Summary and conclusions

In this paper, we have documented the glacioeustatic lowstand-to-highstand transition as recorded in the strata of a shelf margin with a high-sediment supply and high but spatially variable tectonic accommodation. Key surfaces predicted by sequence stratigraphy to mark the progression of relative sea level – sequence boundary, transgressive surface, maximum flooding surface – are identified in the Late Pleistocene and Holocene strata, but their recognition across and along the shelf is difficult due to strong tectonic gradients and the facies they bound are not entirely understood. Characterizing the Waipaoa shelf as accommodation or supply-dominated in the modern eustatic highstand has only local significance: we presented evidence suggesting the two adjacent shelf subbasins fall into each regime, respectively. But when integrated across the entire shelf, our sediment budget combined with paleo-discharge estimates for the Waipaoa River suggest that the middle to late Holocene shelf was accommodation-dominated, as measured by the limited potential for sediment export to the continental slope. This high trapping efficiency appears, however, to be sensitive to sediment supply, since neither long-term nor short-term shelf budgets come close to approximating the elevated, anthropogenically influenced suspended sediment discharge to the coast.

Acknowledgments

This work was supported by the NSF MARGINS Source-to-Sink program (Grant OCE-0405515-02). We thank the crews of the R/V *Kilo Moana* and R/V M*arion Dufresne* for facilitating our fieldwork and helping us with all aspects of data acquisition and core retrieval during the 2005 and 2006 cruises. We also thank Mohammed Sanhaji of EdgeTech for his technical support with the chirp system deployed on the 2005 cruise, and David Amblas for his assistance with the multibeam data and thoughtful suggestions. Thoughtful reviews by Tim Naish, Miquel Canals, and an anonymous reviewer greatly improved the manuscript.

References

Allen, P.A., Allen, J.R., 2005. Basin Analysis: Principles and Applications, 2nd Ed., Blackwell Publishing, 549 p.

Alloway, B.V., Lowe, D.J., Barrell, D.J.A., Newnham, R.M., Almond, P.C., Augustinus, P.C., Bertler, N.A.N., Carter, L., Litchfield, N.J., McGlone, M.S., Shulmeister, J., Vandergoes, M.J., Williams, P.W., NZ-INTIMATE members, 2007. Towards a climate event stratigraphy for New Zealand over the past 30000 years (NZ-INTIMATE project). Journal of Quaternary Science 22 (1), 9–35.

Barnes, P.M., Nicol, A., Harrison, T., 2002. Late Cenozoic evolution and earthquake potential of an active listric thrust complex above the Hikurangi subduction zone, New Zealand. Geological Society of America Bulletin 114 (11), 1379–1405.

Berryman, K., 1993a. Age, height, and deformation of Holocene marine terraces at Mahia Peninsula, Hikurangi subduction margin, New Zealand. Tectonics 12 (6), 1347–1364.

Berryman, K., 1993b. Distribution, age, and deformation of Late Pleistocene marine terraces at Mahia Peninsula, Hikurangi subduction margin, New Zealand. Tectonics 12 (6), 1365–1379.

Berryman, K.R., Ota, Y., Hull, A.G., 1989. Holocene paleoseismicity in the fold and thrust belt of the Hikurangi subduction zone, eastern North Island, New Zealand. Tectonophysics 163, 185–195.

Berryman, K., Marden, M., Eden, D., Mazengarb, C., Ota, Y., Moriya, I., 2000. Tectonic and paleoclimatic significance of Quaternary river terraces of the Waipaoa River, East Coast, North Island, New Zealand. New Zealand Journal of Geology and Geophysics 43, 229–245.

Brown, L.J., 1995. Holocene shoreline depositional processes at Poverty Bay, a tectonically active area, northeastern North Island, New Zealand. Quaternary International 26, 21–33.

Clifton, H.E., Hunter, R.E., Gardner, J.V., 1988. Analysis of eustatic and sedimentologic influences on transgressive and regressive cycles in the upper Cenozoic Merced Formation, San Francisco, California. In: Kleinspehn, K.L., Paola, C. (Eds.), New Perspectives in Basin Analysis. Springer-Verlag, New York, pp. 109–128.

Cochran, U., Berryman, K., Zachariasen, J., Mildenhall, D., Hayward, B., Southall, K., Hollis, C., Barker, P., Wallace, L., Alloway, B., Wilson, K., 2006. Paleoecological insights into subduction zone earthquake occurrence, eastern North Island, New Zealand. Geological Society of America Bulletin 118 (9/10), 1051–1074.

Crosby, B.T., Whipple, K.X., 2006. Knickpoint initiation and distribution within fluvial networks: 236 waterfalls in the Waipaoa River, North Island, New Zealand. Geomorphology 82, 16–38.

Foster, G., Carter, L., 1997. Mud sedimentation on the continental shelf at an accretionary margin — Poverty Bay, New Zealand. New Zealand Journal of Geology and Geophysics 40, 157–173.

Gage, M., Black, R.D., 1979. Slope-stability and geological investigations at Mangatu State Forest. Technical Paper, vol. 66. New Zealand Forest Service, Wellington, NZ. 66 pp.

Gibb, J., 1986. A New Zealand regional Holocene eustatic sea-level curve and its application to determination of vertical tectonic movements. Royal Society of New Zealand Bulletin 24, 377–395.

Gomez, B., Carter, L., Trustrum, N.A., Palmer, A.S., Roberts, A.P., 2004. El Nino-Southern Oscillation signal associated with middle Holocene climate change in intercorrelated terrestrial and marine sediment cores, North Island, New Zealand. Geology 32 (8), 653–656.

Gomez, B., Carter, L., Trustrum, N.A., 2007. A 2400 yr record of natural events and anthropogenic impacts in intercorrelated terrestrial and marine sediment cores: Waipaoa sedimentary system, New Zealand. Geological Society of America Bulletin 119 (11/12), 1415–1432.

Hamilton, E.L., 1971. Prediction of in-situ acoustic and elastic properties of marine sediments. Geophysics 36 (2), 266–284.

Haywick, D., Carter, R.M., Henderson, R.A., 1992. Sedimentology of 40,000 year Milankovitch-controlled cyclothems from central Hawkes Bay, New Zealand. Sedimentology 39, 675–696.

Hicks, D.M., Gomez, B., Trustrum, N.A., 2000. Erosion thresholds and suspended sediment yields, Waipaoa River Basin, New Zealand. Water Resources Research 36 (4), 1129–1142.

Hicks, D.M., Gomez, B., Trustrum, N.A., 2004. Event suspended sediment characteristics and the generation of hyperpycnal plumes at river mouths: East Coast continental margin, North Island, New Zealand. Journal of Geology 112, 471–485.

Kettner, A.J., Gomez, B., Syvitski, J.P.M., 2007. Modeling suspended sediment discharge from the Waipaoa River system, New Zealand: the last 3000 years. Water Resources Research 43, W07411. doi:10.1029/2006WR005570.

Kuehl, S.A., Alexander, C.A., Carter, L., Gerald, L., Gerber, T., Harris, C., McNinch, J., Orpin, A., Pratson, L., Syvitski, J., Walsh, J.P., 2006. Understanding sediment transfer from land to ocean. EOS, Transactions of the American Geophysical Union 87 (29).

Lewis, K.B., 1973. Erosion and deposition on a tilting continental shelf during Quaternary oscillations of sea level. New Zealand Journal of Geology and Geophysics 16, 281–301.

Lewis, K.B., 1980. Quaternary sedimentation on the Hikurangi oblique-subduction and transform margin, New Zealand. In: Balance, P.F., Reading, H.G. (Eds.), Sedimentation in Oblique-Slip Mobile Zones, vol. 4. International Association of Sedimentologists Special Publication, pp. 171–189.

Lewis, K.B., Pettinga, J.R., 1993. South Pacific sedimentary basins. In: Balance, P.F. (Ed.), Sedimentary Basins of the World. Elsevier Science Publishers, Amsterdam, pp. 225–250.

Litchfield, N., Berryman, K., 2007. Relations between postglacial fluvial incision rates and uplift rates in the North Island, New Zealand. Journal of Geophysical Research 111, F02007. doi:10.1029/2005JF000374.

Mazengrab, C., Speden, I.G., 2000. Geology of the Raukumara Area, 1:250,000 Geological Map 6, 1 sheet + 60p. Institute of Geological and Nuclear Sciences, Lower Hutt, NZ.

Mitchum Jr., R.M., Vail, P.R., Sangree, J.B., 1977. Seismic stratigraphy and global changes of sea level, part 6: stratigraphic interpretation of seismic reflection patterns in depositional sequences. In: Payton, C.E. (Ed.), Seismic Stratigraphy — Applications to Hydrocarbon Exploration: American Association of Petroleum Geologists Memoir, vol. 26, pp. 117–133.

Naish, T., Kamp, P.J.J., 1995. Pliocene–Pleistocene marine cyclothems, Wanganui basin, New Zealand: a lithostratigraphic framework. New Zealand Journal of Geology and Geophysics 38, 223–243.

Naish, T., Kamp, P.J.J., 1997. Sequence stratigraphy of sixth-order (41 k.y.) Pliocene–Pleistocene cyclothems, Wanganui basin, New Zealand: a case for the regressive systems tract. Geological Society of America Bulletin 109 (8), 978–999.

Nittrouer, C.A., 1999. STRATAFORM: overview of its design and synthesis of its results. Marine Geology 154, 3–12.

Orpin, A.R., 2004. Holocene sediment deposition on the Poverty-slope margin by the muddy Waipaoa River, East Coast New Zealand. Marine Geology 209, 69–90.

Orpin, A.R., Alexander, C., Carter, L., Kuehl, S., Walsh, J.P., 2006. Temporal and spatial complexity in post-glacial sedimentation on the tectonically active, Poverty Bay continental margin of New Zealand. Continental Shelf Research 26, 2205–2224.

Ota, Y., Berryman, K.R., Hull, A.G., Miyauchi, T., Iso, N., 1988. Age and height distribution of Holocene transgressive deposits in eastern North Island, New Zealand. Palaeogeography, Palaeoclimatology, Palaeoecology 68, 135–151.

Page, M.J., Reid, L.M., Lynn, I.H., 1999. Sediment production form Cyclone Bola landslides, Waipaoa catchment. Journal of Hydrology 38, 289–308.

Pillans, B., Chappell, J., Naish, T.R., 1998. A review of the Milankovitch climatic beat: template for Plio-Pleistocene sea-level changes and sequence stratigraphy. Sedimentary Geology 122, 5–21.

Posamentier, H.W., Allen, G.P., 1999. Siliciclastic sequence stratigraphy — concepts and applications. SEPM Concepts in Sedimentology and Stratigraphy, vol. 7. 204 pp.

Proust, J.N., Lamarche, G., Migeon, S., Neil, H., the shipboard scientific party, 2006. Les Rapport de campagnes a la mer, MD152/MATACORE. Institute Polaire Francais, Plouzane, France. 107 pp.

Reid, L.M., Page, M.J., 2003. Magnitude and frequency of landsliding in a large New Zealand catchment. Geomorphology 49, 71–88.

Please cite this article as: Gerber, T.P., et al., The influence of sea level and tectonics on Late Pleistocene through Holocene sediment storage along the high-sediment supply Waip..., Mar. Geol. (2009), doi:10.1016/j.margeo.2009.10.002

Rosser, B.J., 1997. Downstream fining in the Waipaoa River; an aggrading, gravel-bed river, East Coast, New Zealand, Unpublished MSc thesis, Massey University, Palmerston North, New Zealand, 160 pp.

Schock, S.G., LeBlanc, L.R., Panda, S., 1994. Spatial and temporal pulse design considerations for a marine sediment classification sonar. IEEE Journal of Oceanic Engineering 19 (3), 406–415.

Slingerland, R., Driscoll, N.W., Milliman, J.D., Miller, S.R., Johnstone, E.A., 2007. Anatomy and growth of a Holocene clinothem in the Gulf of Papua. Journal of Geophysical Research 113, FO1S13. doi:10.1029/2006JF000628.

Swift, D.J.P., Thorne, J.A., 1991. Sedimentation on continental margins, I: a general model for shelf sedimentation. In: Swift, D.J.P., Oertel, G.F., Tillman, R.W., Thorne, J.A. (Eds.), Shelf Sand and Sandstone Bodies, vol. 14. International Association of Sedimentologists Special Publication, pp. 3–31.

Széréméta, N., Bassinot, F., Balut, Y., Labeyrie, L., Pagel, M., 2004. Oversampling of sedimentary series collected by giant piston corer: evidence and corrections based on 3.5-kHz chirp profiles. Paleoceanography 19, PA1005. doi:10.1029/2002PA000795.

Vail, P.R., Mitchum Jr., R.M., Thompson III, S., 1977. Seismic stratigraphy and global changes of sea level, part 3: relative changes of sea level from coastal onlap. In: Payton, C.E. (Ed.), Seismic Stratigraphy — Applications to Hydrocarbon Exploration: American Association of Petroleum Geologists Memoir, vol. 26, pp. 63–81.

Walsh, J.P., Alexander, C.A., Gerber, T., Orpin, A.R., Sumners, B.W., 2007. Demise of a submarine canyon? Evidence for highstand infilling on the Waipaoa River continental margin, New Zealand. Geophysical Research Letters 34, L20606. doi:10.1029/2007GL031142.

Walsh, J.P., Nittrouer, C.A., 2003. Contrasting styles of off-shelf sediment accumulation in New Guinea. Marine Geology 196, 105–125.

Wilgus, C.K., Hastings, B.S., Kendall, C.G.St.C., Posamentier, H.W., Ross, C.A., Van Wagoner, J.C., 1988. Sea-Level Changes — An Integrated Approach, vol. 42. SEPM Special Publication. 407 pp.

Wilmshurst, J.M., McGlone, M.S., 1996. Forest disturbance in the central North Island, New Zealand, following the 1850 BP Taupo eruption. Holocene 6 (4), 399–411.

Wood, M.P., 2006. Sedimentation on a high input continental shelf at the active Hikurangi margin, Poverty Bay, New Zealand, Unpublished MSc thesis, Victoria University, Wellington, New Zealand, 199 pp.

Please cite this article as: Gerber, T.P., et al., The influence of sea level and tectonics on Late Pleistocene through Holocene sediment storage along the high-sediment supply Waip..., Mar. Geol. (2009), doi:10.1016/j.margeo.2009.10.002